Sex and chronic stress alter the distribution of glutamate receptors within rat hippocampal CA3 pyramidal cells following oxycodone conditioned place preference

Alexandra Dolgetta [a], Megan Johnson [a], Kate Fruitman [a], Luke Siegel [a], Yan Zhou [b], Bruce S. McEwen [c,1,2], Mary Jeanne Kreek [b,1,3], Teresa A. Milner [a,c,*]

[a] *Feil Family Brain and Mind Research Institute, Weill Cornell Medicine, 407 East 61st Street, New York, NY, 10065, USA*
[b] *The Laboratory of the Biology of Addictive Diseases, The Rockefeller University, 1230 York Avenue, New York, NY, 10065, USA*
[c] *Harold and Margaret Milliken Hatch Laboratory of Neuroendocrinology, The Rockefeller University, 1230 York Avenue, New York, NY, 10065, USA*

ABSTRACT

Glutamate receptors have a key role in the neurobiology of opioid addiction. Using electron microscopic immunocytochemical methods, this project elucidates how sex and chronic immobilization stress (CIS) impact the redistribution of GluN1 and GluA1 within rat hippocampal CA3 pyramidal cells following oxycodone (Oxy) conditioned place preference (CPP). Four groups of female and male Sprague-Dawley rats subjected to CPP were used: Saline- (Sal) and Oxy-injected (3 mg/kg, I.P.) naïve rats; and Sal- and Oxy-injected CIS rats. <u>GluN1</u>: In both naive and CIS rats, Sal-females compared to Sal-males had elevated cytoplasmic and total dendritic GluN1. Following Oxy CPP, near plasmalemmal, cytoplasmic, and total GluN1 decreased in CA3 dendrites of unstressed females suggesting reduced pools of GluN1 available for ligand binding. Following CIS, Oxy-males (which did not acquire CPP) had increased GluN1 in all compartments of dendrites and spines of CA3 neurons. <u>GluA1</u>: There were no differences in the distribution GluA1 in any cellular compartments of CA3 dendrites in naïve females and males following either Sal or Oxy CPP. CIS alone increased the percent of GluA1 in CA3 dendritic spines in males compared to females. CIS Oxy-males compared to CIS Sal-males had an increase in cytoplasmic and total dendritic GluA1. Thus, in CIS Oxy-males increased pools of GluN1 and GluA1 are available for ligand binding in CA3 neurons. Together with our prior experiments, these changes in GluN1 and GluA1 following CIS in males may contribute to an increased sensitivity of CA3 neurons to glutamate excitation and a reduced capacity to acquire Oxy CPP.

1. Introduction

The rate of drug overdose involving synthetic opioids and heroin has risen dramatically, especially in women (Scholl et al., 2018; VanHouten et al., 2019; Strang et al., 2020). Genes, environment (e.g., stress), and multi-drug use are all key factors in the opioid addiction processes in humans (Sinha, 2007; Strang et al., 2020), posing the challenge of elucidating how sex influences this complicated picture. Yet, it has been shown that women may have varying sensitivity to morphine throughout the menstrual cycle (Ribeiro-Dasilva et al., 2011), which

poses the possibility of ovarian hormone involvement in the addictive processes. Furthermore, studies conducted with rodents have shown that various hormones likely have a role in opioid addiction (Becker et al., 2017; Becker and Chartoff, 2019). As an example, varying circulating estrogen levels in rats throughout the estrous cycle has been shown to affect heroin self-administration behaviors (Lacy et al., 2016).

Neural circuits that impact associative memory formation and play a role in encoding motivational incentives serve a crucial role in the pathway of drug addiction for both males and females (Koob and Volkow, 2010). In rodents, associative learning and spatial memory functions are dependent on opioid signaling in the CA3 region of the hippocampus (Meilandt et al., 2004; Kesner and Warthen, 2010). Furthermore, a type of low-frequency opioid-mediated long term potentiation (LTP) has been shown in mossy fiber-CA3 pyramidal cell synapses in proestrus (high estrogen) female rats (Harte-Hargrove et al., 2015). The findings that this opioid mediated LTP is not present in diestrus (low estrogen) female or male rats (Harte-Hargrove et al., 2015) supports the idea that females in certain hormonal states could have increased opioid driven associative learning processes.

Our recent studies have shown that both male and female Sprague-Dawley rats achieve conditioned place preference (CPP) to the mu opioid receptor (MOR) agonist oxycodone (Oxy) (Ryan et al., 2018; Randesi et al., 2019). Anatomical analysis of the hippocampus revealed sex differences in the hippocampal opioid system in a manner that would heighten excitation and opiate associative learning processes to a greater extent in females than in males (Ryan et al., 2018; Bellamy et al., 2019). Notably, within mossy fiber-CA3 synapses, delta opioid receptors (DOR) were repositioned in both Oxy-injected females and males in a pattern that was similar to proestrus females with significant opioid-mediated LTP (Harte-Hargrove et al., 2015; Ryan et al., 2018). In addition, MORs and DORs in hilar interneurons of Oxy-females were redistributed in a way that could enhance granule cell disinhibition via two separate circuits: 1) plasmalemmal associated MORs increased in number in parvalbumin (PARV)-labeled dendrites (Ryan et al., 2018), which function to inhibit granule cell soma (Drake et al., 2007); and 2) plasmalemmal associated DORs increased in number on GABAergic interneuron dendrites (Ryan et al., 2018), which co-localize neuropeptide Y (NPY) and function to promote lateral perforant pathway LTP (Sperk et al., 2007). These changes in the opioid system with Oxy CPP are paralleled by sex-specific changes in the expression and protein density of molecules involved in plasticity (Arc, NPY, BDNF), stress (CRHR1), and related kinase signaling (pAKT, pMAPK) (Randesi et al., 2019).

Another important factor in the mechanism of addiction is stress (Saal et al., 2003; Sinha, 2007). In previous studies, stress has been shown to impact the neural mechanisms of addiction and may influence synaptic plasticity (Saal et al., 2003). Our studies have demonstrated that chronic immobilization stress (CIS) in male rats, but not female rats, down-regulates expression of hippocampal opioid, stress-related, and other signaling molecules that are important for modulating synaptic plasticity (Randesi et al., 2018). Moreover, CIS alters the distribution, phosphorylation, and expression of opioid receptors in the hippocampal pyramidal cells and GABAergic interneurons in a manner that would reduce opioid mediated learning processes in males (Randesi et al., 2018; Bellamy et al., 2019; Reich et al., 2019; Johnson et al 2021; Rubin et al., 2020). These changes in the opioid system likely contribute to our finding that with the addition of CIS, only female, but not male rats, acquired oxycodone CPP (Bellamy et al., 2019; Reich et al., 2019).

Glutamate plasticity has been shown to be involved in the neural circuitry that encode memories important for opioid addictive processes (Heinsbroek et al., 2020). For example, extra-synaptic glutamate in the nucleus accumbens core is increased during heroin reinstatement in male rats (Shen et al., 2014). Moreover, glutamate and opioid receptors co-localize in various regions of the brain that participate in opioid addiction mechanisms (Scavone et al., 2011) including the nucleus accumbens (Wang et al., 1999), central nucleus of the amygdala (Beckerman and Glass, 2012), and the hippocampus (Milner and Drake, 2001). Furthermore, with increasing doses of self-administered morphine in male rats, NMDA receptors, specifically GluN1 labeled subunits, are redistributed from the plasma membrane to the cytoplasm (Glass et al., 2004). AMPA receptors also co-localize with MORs in the central and basal lateral amygdala (BLA) nuclei (Glass et al., 2005; Beckerman and Glass, 2011) and hippocampus (Billa et al., 2010). Moreover, following morphine self-administration or repeated administration, AMPA receptors traffic to the plasma membrane in the BLA (Glass et al., 2005) and hippocampus (Billa et al., 2010). Others have hypothesized that glutamate-opioid interactions are important for adaptations to the chronic use of opioids (Scavone et al., 2011).

Both NMDA and AMPA receptors have been demonstrated to have a role in long term synaptic plasticity (Pál, 2018). Ionotropic NMDA receptors are transmembrane di- or tri-heteromers with a variety of different subunits and can be either extra-synaptic or synaptic in location (Pál, 2018). Synaptic NMDA receptors have been shown to promote cell viability, while extra-synaptic receptors have been shown to promote cell death (Hardingham and Bading, 2010). GluN1 is an essential subunit that is consistently present in the NMDA receptor and associates with other subunits (e.g. GluN2A-D and GluN3A-B) in various combinations (Pál, 2018). The GluN1 subunit has been implicated in contributing to learning and memory in several studies (Rebola et al., 2010). Additionally, the GluN1 subunit is of particular interest as it has been implicated in acute opioid tolerance and hyperalgesia (Zhang et al., 2015). In particular, remifentanil, a short-acting MOR agonist, significantly increases the expression of GluN1 mRNA and phosphorylated-GluN1 protein levels in rat dorsal horn neurons after 1 h of application and lasts for 24 h (Zhang et al., 2015). Furthermore, it has been shown that morphine CPP is associated with increased basal synaptic transmission, impaired hippocampal LTP, and increased synaptic expression of GluN1 and GluN2b subunits in male mice (Portugal et al., 2014). As these studies have demonstrated that the GluN1 subunit is impacted by opioid administration, we sought to uncover if GluN1 subunit trafficking is impacted by Oxy CPP and/or chronic stress.

The AMPA glutamate receptor plays a key role in mediating excitatory postsynaptic currents at glutamatergic synapses [reviewed in (Sheng and Kim, 2002)]. Similar to NMDA receptors, AMPA receptors are ionotropic glutamate receptors that are essential for excitatory transmission and participate in hippocampal synaptic plasticity (Barkóczi et al., 2012). AMPA receptors are tetramers composed of diverse combinations of GluA1-4 subunits, each of which express various biophysical properties. The receptor subunit GluA1 has been robustly studied as it has been shown to be vital to synaptic plasticity by transporting and incorporating the AMPA receptor into synaptic membranes of neurons (Frey et al., 2009; Barkóczi et al., 2012; Zhang and Abdullah, 2013). LTP induces the distribution of AMPA receptors containing GluA1 into the synapses of hippocampal CA1 pyramidal cells in rats (Hayashi et al., 2000). GluA1 has been shown to have non-detectable effects on the basal synaptic transmission between rat hippocampal neurons, but when the receptor was mutated it was shown that LTP is blocked, demonstrating that the presence of GluA1 containing AMPA receptors is a significant mechanism in potentiating LTP and plasticity (Hayashi et al., 2000).

Several studies have shown that the synaptic transmission of glutamate, specifically through NMDA and AMPA receptors, is a key mechanism in the neurobiology of drug addiction and pain modulation (Hou et al., 2009). Yet, the mechanism of how this occurs and which functional areas of the brain are involved is poorly understood. The current study looks to expand the understanding of how these two glutamate receptor subunits are impacted in the hippocampus following opioid-associative learning processes. Specifically, we analyzed the redistribution of GluN1 and GluA1 in hippocampal CA3 pyramidal cells of naïve and CIS rats following oxycodone CPP using light and electron microscopic (EM) immunocytochemical methods.

2. Materials & methods

2.1. Animals

This study used tissues from two cohorts of adult Sprague-Dawley rats (N = 48; RGD Cat# 734476, RRID:RGD_734476) that were collected in our previous studies (Mazid et al., 2016; Ryan et al., 2018; Reich et al., 2019). The adult rats were approximately 2.5 months old upon arrival, and males weighed 275–325 g and females were 225–250 g. Cohort 1. Saline-injected (Sal) naïve females and males or Oxy-injected naïve females and males that were subjected to CPP (N = 6/group) (Ryan et al., 2018). Cohort 2. CIS Sal-females and males or CIS Oxy-females and males that were subjected to CPP (N = 6/group) (Reich et al., 2019). Rats were single-housed in R20 rat cages (10.5 in x 19 in x 8 in; Ancare, Bellmore NY) with a 12-h light/dark cycle (lights on 0600–1800) and *ad libitum* access to water and food. All animal procedures approved by the Weill Cornell Medicine and Rockefeller University Institutional Animal Care and Use Committees and were in accordance with the 2011 Eighth edition of the National Institutes of Health Guidelines for the Care and Use of Laboratory Animals.

2.2. Animal experimentation

Handling and Estrous Cycle Determination: Handling can have significant effects on stress as measured by corticosterone levels (Deutsch-Feldman et al., 2015; Collins et al., 2016). To minimize stress, rats were acclimated to the animal facilities for one week and then gently handled for 3–5 min per day for 5 days prior to beginning experiments. Rats in each cohort were handled by the same experimenters for the CPP behavior (cohorts 1 and 2) and CIS procedure (cohort 2). To minimize experimental variability, behaviors and euthanasia was performed on each cohort of female and male rats at the same time of day. Behavior occurred in the morning and euthanasia was always performed immediately after the last CPP section, between 9:00 a.m. and 1:00 p.m. for all rats (Ryan et al., 2018; Reich et al., 2019). All female rats used in this study were in the estrus phase of the estrous cycle (Ryan et al., 2018; Reich et al., 2019), as assessed by vaginal smear cytology (Turner and Bagnara, 1971) on the day of euthanasia, after the rats were anesthetized and prior to aortic perfusion (described below).

CIS: Rats were subjected to CIS for 10 consecutive days (Mazid et al., 2016; Reich et al., 2019). For CIS, rats were placed in plastic cone shaped polyethylene bags containing a small hole at the apex and a Kotex mini-pad for urine collection. For 30 min each day, the rats were placed with their noses protruding from the hole in the bag, the bags were sealed in with tape and left undisturbed. The rats started CPP training two days following the last stress period.

Oxycodone CPP: The CPP apparatus (product # MED-CPP-013, MED Associates Inc) is comprised of distinct compartments (white, black and a neutral central gray) separated by removable doors. The CPP protocol followed a 14-day sequence: 1) preconditioning (day 1): Rats were allowed free access to the entire apparatus for 30 min. As rats in each cohort had a side preference (Ryan et al., 2018; Reich et al., 2019), oxycodone was administered in the nonpreferred side during conditioning (i.e., biased CPP design). 2) conditioning (day 2-9): Rats underwent 4 training sessions. On the first day of each session, the rats were injected with oxycodone (3 mg/kg, i.p.) and confined in one compartment (e.g., black) for 30 min (a time point within the 3–5 h half-life of oxycodone (Ordonez Gallego et al., 2007)). On the second day of each session, the rats were injected with saline and confined in the other compartment (e.g., white) for 30 min. Control rats received saline prior to both conditioning sessions. 3) CPP test (day 14): Four days following the last injection, the rats were placed in the central gray compartment and allowed free access to the entire apparatus with their behavior monitored for 30 min. Percent time in the Oxy-paired compartment was calculated by dividing the time spent in the Oxy-paired compartment over the time spent in both compartments.

Preference score was calculated by subtracting the percent time in the Oxy-paired compartment during the pre-test from that of the post-test. Our previous studies demonstrated that the naïve female and male rats used in these experiments (cohort 1) both acquired oxycodone CPP (Ryan et al., 2018). There were significant increases in percent time spent in the Oxy-paired chamber in both naïve females and males, with a greater increase in female rats; moreover, Oxy-males had a significant decrease in locomotion score in the first three training sessions (Ryan et al., 2018). Only the CIS female rats used in these experiments (cohort 2) acquired Oxy CPP (Reich et al., 2019). In particular, CIS females had a significant increase in the percent change in preference score for the Oxy-associated chamber whereas the CIS males did not; however, there were no significant differences in locomotion in CIS females or males in any of the four training sessions regardless of treatment (Reich et al., 2019).

2.3. Antibody characterization

GluA1: A polyclonal rabbit antibody raised against the cytoplasmic domain of GluA1 (AB_1504, Millipore Sigma, Billerica MA) was used. On Western blots this antibody recognizes one major band at ~106 kD on 10 μg of mouse brain lysate [manufacturer's data sheet, www.emdmillipore.com and (Yokoi et al., 2016)]. Additionally, Western blots, immunoprecipitation, and electron microscopic localization of GluA1 immunoreactivity in rat hippocampus demonstrate the expected locations in pre- and post-synaptic profiles (Hussain et al., 2015).

GluN1: A monoclonal mouse antibody against GluN1 (the NMDAR1 protein encoded by the Grin1 gene) was used (clone 54.1; RRID: AB_86917; BD Biosciences, San Diego, CA). Reduced immunoreactivity for this antibody has been shown following rAAV-Cre injection into a targeted brain regions in floxed GuN1 mice (Glass et al., 2008). Specificity of the GluN1 antibody was demonstrated by immunoprecipitation and immunohistochemistry (Brose et al., 1994; Siegel et al., 1994, 1995). On Western blots of rat synaptic membranes and monkey hippocampal homogenates, the GluN1 antibody yields in one major band at ~116 kD. HEK 293 cells transfected with cDNA encoding GluN1 show similar results, whereas non-transfected cells yield in no bands (Siegel et al., 1994).

PARV: Two PARV antibodies were used. When combined with GluA1, a mouse monoclonal PARV antibody (Sigma-Aldrich Cat#P3088, RRID:AB_477329) was used. The specifics of this antibody have been shown by immunoblots and radioimmunoassay in brain tissue (Celio et al., 1988; Celio, 1990). When combined with GluN1, a polyclonal rabbit anti-PARV against rat muscle PARV (provided by Dr. K.G. Baimbridge, University of British Columbia, Vancouver) was used. Its specificity has been demonstrated western blots of rat brain and muscle soluble proteins yields a single band which corresponds to rat muscle PARV (Mithani et al., 1987). Moreover, this antiserum was shown to have no cross-reactivity with other calcium-binding proteins (Mithani et al., 1987). Preincubation of this antibody with 10 ng/ml rat muscle PARV completely abolished immunolabeling in the hippocampus (Sloviter, 1989).

2.4. Immunocytochemical procedures

The details for section preparation and dual labeling immunocytochemistry are described previous (Milner et al., 2011).

Section preparation: The rats were anesthetized with ketamine (100 mg/kg) and xylazine (10 mg/kg) I.P. and perfused through the ascending aorta sequentially with: 1) 10–15 ml 0.9% saline and 2% heparin; 2) 50 ml 3.75% acrolein and 2% paraformaldehyde (PFA) in 0.1 M phosphate buffer (PB; pH7.4); 3) 200 ml 2% PFA in PB. Coronal sections (40 μm thick) through the hippocampus were cut on a Vibratome and stored in cryoprotectant solution (30% sucrose, 30% ethylene glycol in PB) at −20 °C until use. To ensure identical labeling conditions between groups, tissue sections were coded with hole-punches in the

cortex and processed in a single container throughout the immunocytochemical procedures (Milner et al., 2011). Sections were incubated in 1% sodium borohydride in PB for 30 min to neutralize reactive aldehydes (Milner et al., 2011) then rinsed in PB 8–10 times until the gaseous bubble disappeared.

Dual labeling EM immunocytochemistry: The sections were washed in 0.1M Tris-buffered saline (TS; pH7.6) and blocked for 30 min in 0.5% bovine serum albumin (BSA) in TS. Tissue sections were put in a mixture of primary antibodies in 0.1% BSA in TS: mouse anti-GluN1 (1:50) + rabbit anti-PARV (1:5000) or rabbit anti-GluA1 (1:150) + mouse anti-PARV (1:2500). For 24 h, sections were kept on a shaker at room temperature for 24 h and then at 4 °C for four days. Next, the tissue sections were prepared for peroxidase labeling for PARV. For this, sections were rinsed in TS and incubated in a 1:400 dilution of either biotinylated donkey-anti-rabbit IgG (for GluN1; Jackson Immunoresearch Laboratories, Cat# 711-506-152, RRID:AB_2616595) or biotinylated donkey-anti-mouse (for GluA1; Vector Laboratories Cat# BA-2001; RRID:AB_2336180) for 30 min. Sections were incubated in avidin-biotin complex (ABC; Vectastain elite kit, Vector Laboratories, Burlingame, CA) at half the manufacturer's recommended dilution for 30 min, rinsed in TS, and reacted in 3,3′-diaminobenzidine (DAB; Sigma-Aldrich, St. Louis, MO) in 3% H_2O_2 in TS for 7 min (GluN1) or 11 min (GluA1) and rinsed in TS. Tissue sections were rinsed in TS followed by PB and then incubated at 4 °C overnight in a 1:50 dilution of either goat anti-mouse IgG conjugated to 1-nm gold particles [for GluN1; Electron Microscopy Sciences (EMS) Cat# 810.311, RRID:AB_2629850] in 0.01% gelation and 0.08% BSA dissolved in 0.01M phosphate-buffered saline (PBS). Sections were rinsed in PBS and post-fixed for 10 min in 2% glutaraldehyde in PBS. Next, they were rinsed in PBS then by 0.2M sodium citrate buffer (pH = 7.4). IgG-conjugated gold particles were enhanced for 15.5 min (GluA1) or 19.5 min (GluN1) with a silver solution [SEKL15 Silver enhancement kit, Prod No. 15718 Ted Pella Inc.].

Sections were fixed in 2% osmium tetroxide in PB for 1 h and subsequently washed in PB and dehydrated using increasing concentrations of ethanol followed by propylene oxide. The sections were embedded in EMBed 812 (EMS, Cat #14120). Ultrathin sections (approximately 70–72 nm thick) through the CA3b region (Fig. 1A) were cut on a Leica ultratome and collected on 400 mesh thin-bar copper grids (EMS, T400-Cu), which then were counterstained with Uranyless™ (EMS, #22409) and lead citrate (EMS, #22410).

2.5. EM data collection and analysis

Identification of EM profiles: Investigators who were blind to the experimental condition [saline injected (Sal) or Oxy CPP (Oxy)] compiled and evaluated the data. Once figures were created, the experimental condition was unblinded. Tissue sections containing the hippocampal CA3 region were analyzed on a Tecnai transmission electron microscope (FEI, Hillsboro, OR, USA). Images were taken at a magnification of 13,500×, and cells were identified as neuronal or glial using standard morphological criteria (Peters et al., 1991). Dendrites were post-synaptic to axon terminals and also were subdivided as large (diameter >1.0 μm) or small (diameter <1.0 μm). Axon terminals contained numerous small synaptic vesicles. In addition to the existence of multiple small synaptic vesicles, mossy fiber terminals in stratum lucidum (SLu) were large (approximately 1.5–2 μm in diameter) (Pierce et al., 2014) (Pierce et al., 2014). Immunoperoxidase in PARV-containing dendrites appeared as an electron-dense precipitate and silver-intensified immunogold (SIG) labeling for GluA1 or GluN1 appeared as a black electron-dense particles (Milner et al., 2011).

Analysis 1: dendritic profiles in CA3 SR. Dendrites containing either GluA1-SIG or GluN1-SIG-labeled dendrites were photographed from stratum radiatum (SR) of CA3 and analyzed as described previously (Mazid et al., 2016). Dendrites dually labeled with PARV were omitted from the analysis. Photographs were taken of 50 randomly selected single-labeled dendrites, and the subcellular localization of the GluA1-or GluN1-SIG particles was ascertained. As discussed in our prior publication (Ryan et al., 2018), previous studies have established that 50 dendritic profiles per block are adequate to make numerical comparisons on sub-cellular distribution of proteins between groups. Microcomputer Imaging Device software (MCID; RRID:SCR_014278) was utilized to analyze the perimeter, major and minor axis lengths, diameter and cross-sectional area for each dendrite.

The subcellular localization of GluA1-and GluN1-SIG labeling was analyzed using several parameters: (1) the number of SIG particles on the plasmalemma of the dendrite (PM:μm), (2) the number of SIG particles localized within 50 nm of the plasmalemma (Near PM:μm), (3) the number of SIG particles localized to the cytoplasm per cross-sectional area (CY:$μm^2$), and (4) the total number of SIG particles per cross-sectional area (Total:$μm^2$). To calculate the partitioning ratio, the number of SIG particles in a given subcellular compartment (i.e., on plasma membrane (PM), near PM, or in the cytoplasm) was divided by the total number of DOR or MOR-SIG particles in the cell.

Different localizations of SIG particles indicate different functions. SIG labeling on the plasma membrane indicates receptor-binding sites while labeling near the plasma membrane indicates a pool of receptors that can be placed on or taken off of the plasma membrane (Boudin et al., 1998; Ladépêche et al., 2014). SIG labeling in the cytoplasm indicates receptors that are either in the process of being degraded or recycled, or receptors that are being stored during relocation to or from the soma or another cellular subdivision (Pierce et al., 2009; Fernandez-Monreal et al., 2012). Following agonist stimulation, the ratio of
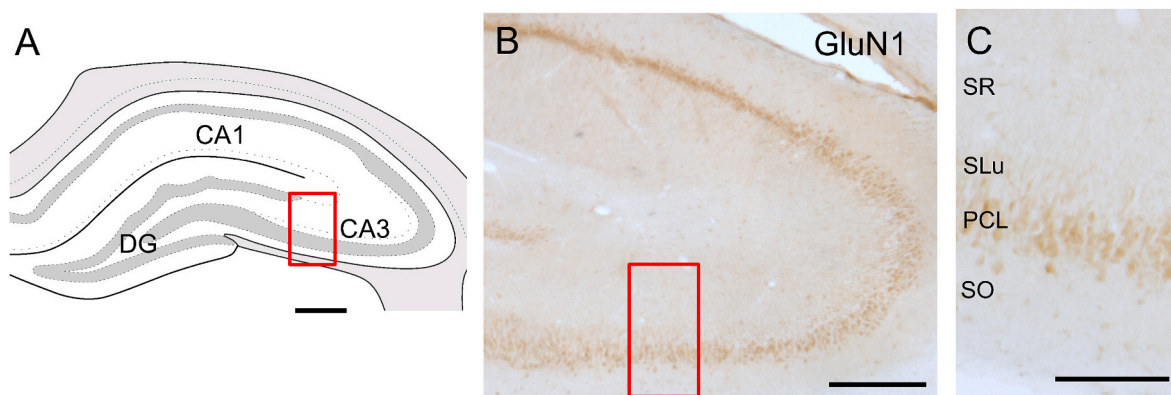
Fig. 1. Hippocampal region sampled for electron microscopy. **A.** Schematic diagram of the rostral rat hippocampus showing the CA1, CA3 and dentate gyrus subregions. CA3 (boxed region) was sampled for electron microscopy [modified from diagram 31 (−3.70 from bregma) in (Swanson, 1992)]. **B.** By light microscopy, dense GluN1-immunoreactivity is seen in the pyramidal cell layer (PCL) and to a lesser extent in stratum oriens (SO), stratum lucidum (SLu) and stratum radiatum (SR). Scale bar = 0.5 mm.

receptors on the plasma membrane to those in the cytoplasm declines, as illustrated by the number of SIG-labeled receptors in each cellular compartment (Haberstock-Debic et al., 2003).

Analysis 2: GluA1-or GluN1-labeled dendritic spines in CA3 SR. One hundred spine profiles per rat were selected randomly from SR (same micrographs used in analysis 1). Spines selected were contacted by terminals forming asymmetric synapses and were categorized as labeled (at least 1 SIG particle) or unlabeled. SIG particles in labeled spines were classified as at the synapse, on the plasma membrane, or in the cytoplasm.

Analysis 3: GluA1-or GluN1-labeled dendritic spines contacted by mossy fibers. The number of GluA1-and GluN1-SIG-labeled dendritic spines contacted by mossy fibers in SLu of CA3 was examined as in prior studies (Harte-Hargrove et al., 2013; Mazid et al., 2016). Photographs were taken of 50 randomly selected mossy fibers in contact with spines from the tissue-plastic interface. Both the percentage of labeled spines (i. e., spines containing 1 or more SIG particle) and location of the SIG particle in the spine (at the synapse, on the plasma membrane, in the cytoplasm) were recorded.

2.6. Figure preparation

Modifications to images were applied uniformly to the entire image. There was no specific portion of the images were introduced, extracted, augmented, concealed or relocated. EM images were initially opened in Adobe Photoshop 9.0 (Adobe Photoshop, RRID:SCR_014199), where resolution was increased (400 dpi) and alterations for contrast, brightness, and sharpness (using unsharp mask) were done. For final layout and labeling, all images were transferred to Microsoft Powerpoint 2010. Supplementary adjustments to brightness and contrast were made in Powerpoint in order to keep the appearance of micrographs consistent. Ultimately, graphs were produced using Prism 7 software (Graphpad Prism, RRID:SCR_002798).

2.7. Statistical analysis

All statistical analyses were conducted on JMP 12 Pro software (JMP, RRID:SCR_014242) unless mentioned otherwise. Significance was set to an alpha <0.05. Statements such as "trending interactions" and "verging on significance" were used to describe data with an alpha of 0.06–0.08. Data are expressed as mean ± SEM. The distribution of SIG particles in dendrites (analysis 1) was analyzed using a two-way analysis of variance (ANOVA) followed by a Tukey post hoc. A Student's t-test was used to compare the number of GluA1 or GluN1-labeled spines (analyses 2 and 3) between groups. To be noted, there were no significant differences in the distribution of GluN1 or GluA1 in small dendrites of any experimental groups besides those seen in Fig. 11.

3. Results

3.1. GluN1 results

3.1.1. COHORT 1. GluN1 distribution in CA3 dendrites from naïve rats following Oxy CPP

Sal-females have elevated dendritic GluN1 in most cellular compartments compared to other groups.

At the light microscopic level, dense GluN1 labeling was detected in the CA3 pyramidal cell layer and to a lesser extent in stratum oriens (SO), stratum lucidum (SLu) and stratum radiatum (SR) (Fig. 1B). Representative electron micrographs showing GluN1-SIG labeling in CA3 pyramidal cell dendrites in SR for all four groups are shown in Fig. 2A–D. GluN1-SIG particles were found on the plasma membrane, near the plasma membrane and in the cytoplasm of CA3 dendrites.

Two-way ANOVA showed significant main effects of condition (Sal vs Oxy) on GluN1-SIG particle density near the plasma membrane ($F_{3,596} = 5.54$; $p = 0.02$), in the cytoplasm ($F_{3,596} = 7.75$; $p = 0.03$), and in total ($F_{3,596} = 11.34$; $p = 0.05$) in CA3 dendrites in naïve rats (cohort 1). Significant sex by condition interactions for GluN1-SIG densities in CA3 dendrites were found near the plasma membrane ($F_{3,596} = 5.54$; $p = 0.0009$), in the cytoplasm ($F_{3,596} = 7.75$; $p < 0.0001$), and in total
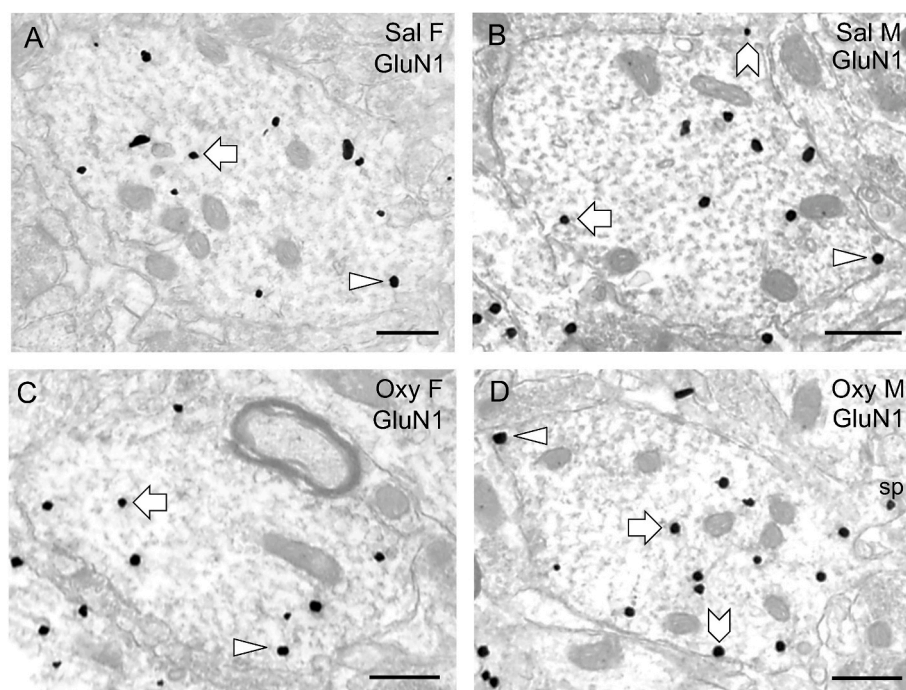
Fig. 2. Representative electron micrographs of GluN1-SIG particles in CA3 pyramidal cell dendrites in naïve Sal- and Oxy-female and male rats. A-D. Electron micrographs show the distribution of GluN1-SIG particles within dendrites from a Sal-female (**A**), a Sal-male (**B**), an Oxy-female (**C**), and an Oxy-male (**D**) rat. Examples of near plasmalemmal (triangle) and cytoplasmic (arrow) DOR-SIG particles in dendrites are shown. Scale bar = 500 nm.

($F_{3,596} = 11.34$; $p < 0.0001$). Post hoc analysis showed a greater dendritic density of GluN1-SIG particles in the cytoplasm ($p = 0.0008$) and in total ($p = 0.0001$) in Sal-females compared to Sal-males (Fig. 3A and B). Oxy-females compared to Sal-females had fewer GluN1-SIG particles near the plasma membrane ($p = 0.0005$), in the cytoplasm ($p < 0.0001$), and in total ($p < 0.0001$) in CA3 dendrites (Fig. 3A). Compared to Oxy-females, Oxy-males had greater GluN1-SIG densities near the plasma membrane ($p = 0.03$) and in total in CA3 dendrites ($p = 0.003$) (Fig. 3A and B).

Significant differences in GluN1 distributions were seen when grouping the CA3 dendrites by size, specifically in the large CA3 dendrites. Two-way ANOVA showed a main effect of treatment (Sal vs Oxy) in the density of GluN1-SIG particles near the plasma membrane ($F_{3,385} = 3.91$; $p = 0.03$) and in total ($F_{3,385} = 7.33$; $p = 0.03$) in large CA3 dendrites. There was a main effect of sex and condition (Sal vs Oxy) on GluN1-SIG particle density on the plasma membrane ($F_{3,385} = 3.91$; $p = 0.03$), in the cytoplasm ($F_{3,385} = 8.44$; $p = <0.0001$), and in total ($F_{3,385} = 7.33$; $p < 0.0001$) of large CA3 dendrites. Post hoc analysis showed a greater dendritic density of GluN1-SIG particles in large CA3 dendrites of Sal-females in the cytoplasm ($p = 0.0008$) and in total ($p = 0.006$) compared to Sal-males (Fig. 3C and D). There was a greater dendritic density of GluN1-SIG particles near the plasma membrane ($p = 0.01$), in the cytoplasm ($p < 0.0001$), and in total ($p < 0.0001$) in large CA3 dendrites of Sal-females compared to Oxy-females (Fig. 3C). Oxy-males compared to Oxy-females had a greater density trending significance of GluN1-SIG particles near the plasma membrane ($p = 0.07$), and had significantly greater density in the cytoplasm ($p = 0.03$) and in total ($p = 0.04$) of large CA3 dendrites (Fig. 3C and D).

There was no significant data for partitioning ratios of GluN1-SIG particles in CA3 dendrites when examined in total. When dendrites were separated by size, there was a significant interaction between sex and condition in the partitioning ratios of GluN1-SIG particles on the plasma membrane of large CA3 dendrites ($F_{3,385} = 2.64$; $p = 0.04$). Post hoc analysis showed that the proportion of GluN1 on the plasma membrane of large CA3 dendrites tended to be greater ($p = 0.08$) in Oxy-females compared to Oxy-males (Fig. 3E and F).

3.2. Sal-females have elevated plasma membrane associated GluN1 in dendritic spines

GluN1-SIG particles were found in dendritic spines in CA3 SR (Fig. 4A and B) and SLu (Fig. 4C). The percentage of GluN1-containing spines in SR was similar in all four groups (Table 1). However, Sal-female rats had significantly more GluN1-SIG particles on the plasma membrane of SR spines compared to Sal-males ($p = 0.02$) and Oxy-females ($p = 0.03$). The percent of GluN1-labeled dendritic spines
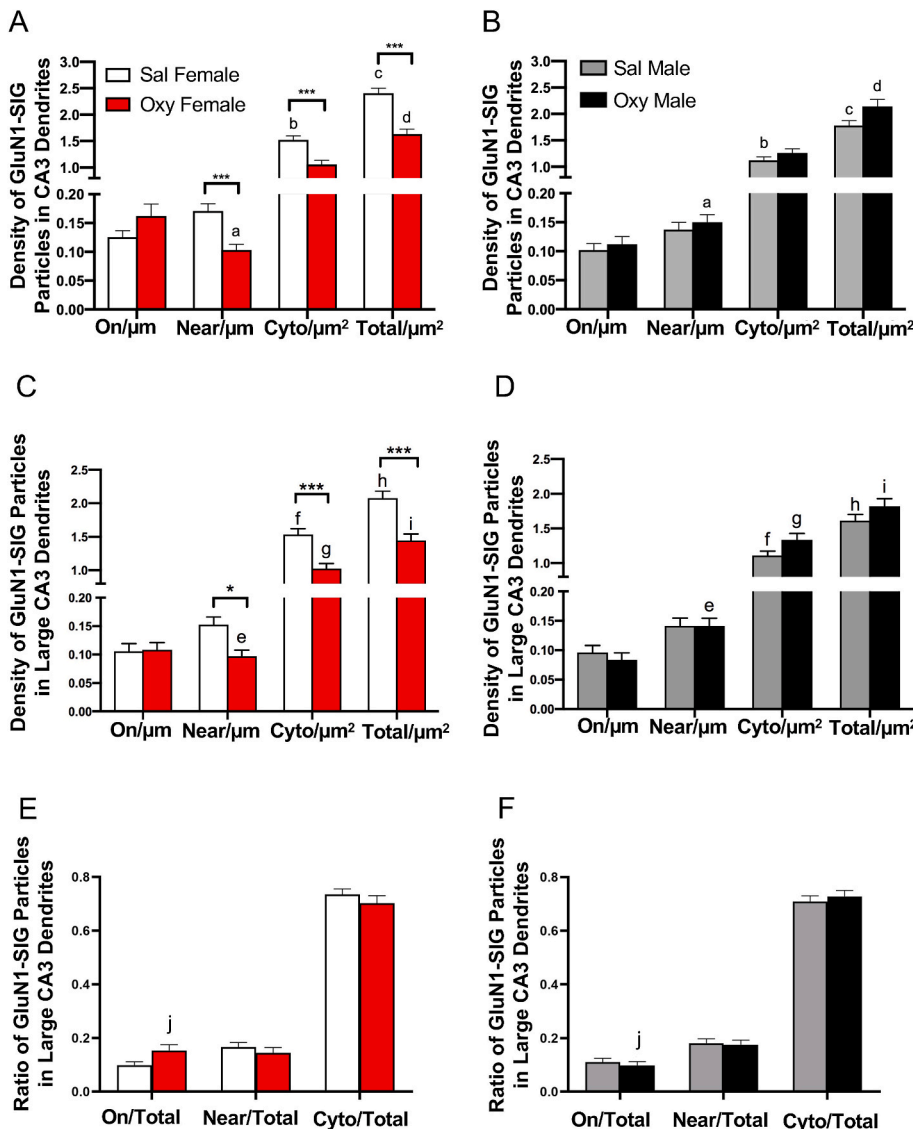

Fig. 3. Quantitative analysis of the distribution of GluN1-SIG particles in CA3 pyramidal cell dendrites in naïve Sal- and Oxy-female and male rats. A, B. Sal-females compared to Sal-males have a greater density of GluN1-SIG particles in the cytoplasm and in total in CA1 pyramidal cell dendrites. Sal-females compared to Oxy-females had greater GluN1-SIG particles near the plasma membrane, in the cytoplasm, and in total in CA3 dendrites (A). Oxy-females compared to Oxy-males have a decreased density of GluN1-SIG particles near the plasmalemma and in total. C, D. When dendrites are divided on the basis of size, Sal-females compared to Sal-males have a greater density of GluN1-SIG particles in the cytoplasm and in total in large CA3 dendrites. Sal-females compared to Oxy-females have a greater density of GluN1-SIG particles near the plasma membrane, in the cytoplasm, and in total in large CA3 dendrites (C). Oxy-females compared to Oxy-males have a decreased density of GluN1-SIG particles near the plasma membrane, in the cytoplasm, and in total in large CA3 dendrites. E, F. Oxy-females compared to Oxy-males have a greater ratio of GluN1-SIG particles in large CA3 dendrites. ***$p < 0.001$, **$p < 0.01$, *$p < 0.05$, $p^{b,c,f} < 0.001$, $p^{d,h} < 0.01$, $p^{a,g,i} < 0.05$, $p^e = 0.05$, N = 3 rats per group; n = 50 dendrites per rat.
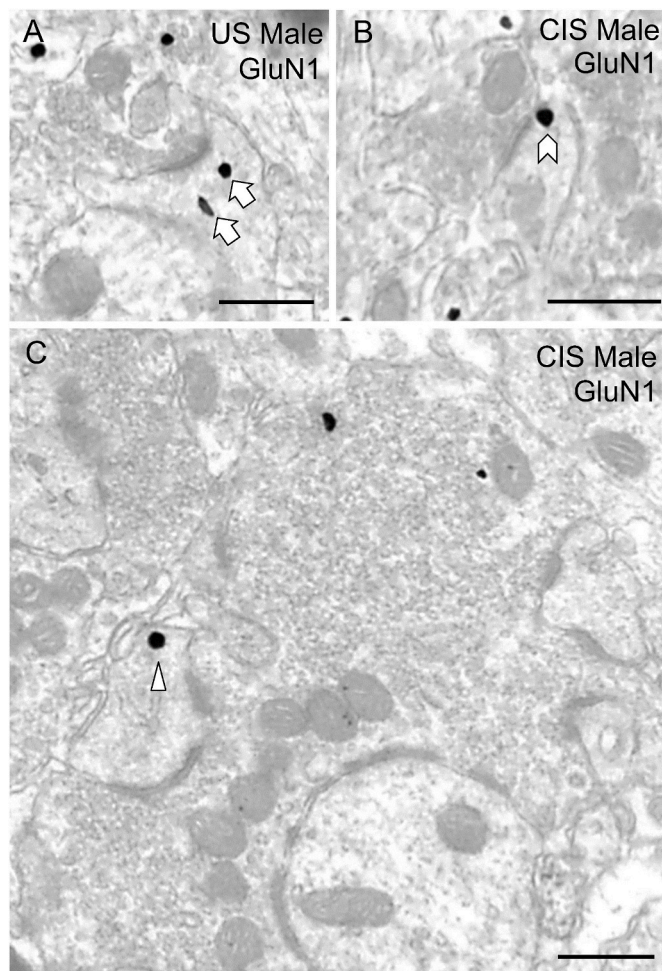
Fig. 4. Examples of GluN1-labeled spines in CA3. Usually one GluN1-SIG particle was found in a single dendritic CA3 spine, but sometimes more than one was detected. **A**. A CA3 spine in the SR of an unstressed (US) male contains two GluN1-SIG particles in the cytoplasm (arrows). **B**. A GluN1-SIG particle on the synapse (chevron) in a SR spine of a CIS male. Both spines are contacted by unlabeled terminals (uT) **C**. A GluN1-SIG particle is found near the plasma membrane (arrowhead) of a CA3 spine contacted by a mossy fiber (MF) in the SLu. Scale bar: 500 nm.

Table 1
GluN1-labeled spines in CA3.

Group	% ± SEM labeled spines	Location*		
		synapse	membrane	cytoplasm
CPP SR				
Male Sal	10.33 ± 3.18	1.67 ± 1.20	**1.0 ± 0.58**[a]	7.0 ± 2.0
Male Oxy	9.33 ± 3.18	0.33 ± 0.33	3.0 ± 0.58	6.0 ± 1.73
Female Sal	14.33 ± 4.18	0.33 ± 0.33	**6.0 ± 2.08**[a,b]	11 ± 3.61
Female Oxy	10.67 ± 6.67	1.33 ± 1.33	**0.67 ± 0.67**[b]	9.33 ± 5.33
CPP SLu				
Male Sal	13.33 ± 4.33	1.67 ± 0.67	4.0 ± 2.08	9.67 ± 3.38
Male Oxy	11.33 ± 3.93	0.33 ± 0.33	4.33 ± 0.88	8.33 ± 4.91
Female Sal	14 ± 3.21	2.67 ± 1.20	4.67 ± 2.33	6.67 ± 1.20
Female Oxy	12.67 ± 5.70	0.67 ± 0.33	2.67 ± 0.33	11 ± 7.02
CIS + CPP SR				
Male Sal	**4.0 ± 1.0**[c]	0.33 ± 0.33	1.33 ± 0.33	**2.33 ± 0.33**[d]
Male Oxy	**12.33 ± 1.76**[c]	0.67 ± 0.33	3.33 ± 0.67	**10.67 ± 2.03**[d]
Female Sal	8.0 ± 1.15	0.33 ± 0.33	2.0 ± 1.0	5.67 ± 1.67
Female Oxy	9.67 ± 1.76	1.0 ± 0.58	4.0 ± 2.0	6.67 ± 1.20
CIS + CPP SLu				
Male Sal	6.67 ± 1.45	**0**[e]	3.0 ± 0.58	3.67 ± 1.20
Male Oxy	13.0 ± 4.16	**3.67 ± 1.86**[e]	3.33 ± 1.45	8.67 ± 2.91
Female Sal	10.0 ± 1.15	1.33 ± 0.88	4.0 ± 0.58	5.0 ± 1.53
Female Oxy	9.33 ± 1.86	0.67 ± 0.67	3.33 ± 0.67	7.33 ± 1.20

a: *p = 0.0163; b: *p = 0.1020; c: **p = 0.0038; d: **p = 0.0037; e: *p = 0.0432.
*Some spines had more than one GluN1-SIG particle.

contacted by mossy fibers (Table 1) was not significantly different between the four groups.

In summary, females compared to males had higher baseline levels of cytoplasmic GluN1 in CA3 dendrites as well as GluN1-containing dendritic spines in SR. However, Oxy CPP primarily alters the distribution of GluN1s within CA3 dendrites in females but has little effect in males. In particular, in Oxy-females compared to males, GluN1s are decreased near the plasma membrane of CA3 dendrites as well as on the plasma membrane of SR spines. This finding suggests that Oxy CPP in females, but not males, results in a decreased availability for GluN1 binding to glutamate in CA3 dendrites.

3.3. COHORTS 1 & 2. GluN1 distribution in CA3 dendrites from Sal naïve compared to CIS rats

3.3.1. GluN1 redistributes to the cytoplasm in CA3 dendrites of CIS Sal-females

Next, the distributions of GluN1 in SR dendrites were compared between the unstressed (US; naïve) and CIS Sal-females and Sal-males. Two-way ANOVA showed a main effect of condition (US vs CIS) in the density of plasma membrane GluN1-SIG particles ($F_{3,596} = 4.76$; p =

0.0006) in CA3 dendrites. There was also a main effect of sex ($F_{3,596} = 17.89$; p < 0.0001) and condition ($F_{3,596} = 17.89$; p < 0.0001) in the density of cytoplasmic GluN1-SIG particles in CA3 dendrites. Additionally, there was a main effect of sex ($F_{3,596} = 18.31$; p < 0.0001) and condition ($F_{3,596} = 18.31$; p < 0.0001) of total GluN1-SIG particle density in CA3 dendrites. Post hoc showed that CIS Sal-females compared to US Sal-females had lower densities of GluN1-SIG particles on the plasma membrane (p = 0.003) of CA3 dendrites and higher densities of GluN1-SIG particles in the cytoplasm (p = 0.0003) and in total (p = 0.002) in CA3 dendrites (Fig. 5A). CIS Sal-males compared to US Sal-males similarly had more total GluN1-SIG particles in CA3 dendrites (p = 0.004) (Fig. 5B). Also, CIS Sal-females compared to CIS Sal-males had more GluN1-SIG particles in the cytoplasm (p < 0.0001) and in total (p = 0.0005) in CA3 dendrites (Fig. 5A and B). US Sal-females compared to US Sal-males had a greater density of GluN1-SIG particles in the cytoplasm (p = 0.01) and in total (p = 0.0009) in CA3 dendrites (Fig. 5A and B).

The percentage of GluN1 labeled spines was not significantly different in US Sal-females compared to CIS Sal-females nor in US Sal-males compared to CIS Sal-males in either the SR or SLu (Table 1).

In summary, total GluN1 within CA3 dendrites increased in both females and males following CIS. Moreover, CIS redistributed GluN1 away from the plasma membrane of CA3 dendrites in females and from SR dendritic spines in males. These findings suggest that CIS reduces availability of GluN1 binding capacity in CA3 neurons in both females and males albeit at different cellular locations.
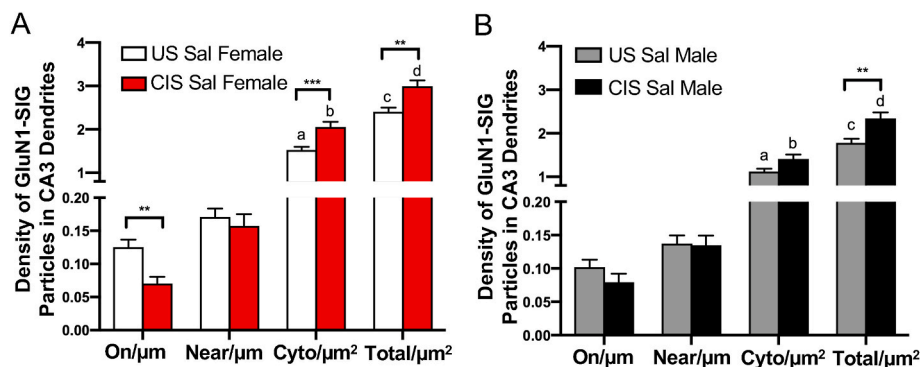
Fig. 5. Quantitative analysis of the distribution of GluN1-SIG particles in CA3 pyramidal cell dendrites in unstressed (US) and CIS Sal-female and Sal-male rats. **A,B.** US Sal-females compared to US Sal-males have a greater density of GluN1-SIG particles in the cytoplasm and in total in CA3 dendrites. After undergoing CIS, females (**A**) have a greater density of GluN1-SIG particles in the cytoplasm and in total in CA3 dendrites, but a decreased density of GluN1-SIG particles on the plasma membrane. After undergoing CIS, males (**B**) have a greater density of GluN1-SIG particles in total in CA3 dendrites. CIS Sal-females compared to CIS Sal-males have a greater density of GluN1-SIG particles in the cytoplasm and in total in CA3 dendrites. ***$p < 0.001$, **$p < 0.01$, *$p < 0.05$, $P^a < 0.05$, $p^{b,c,d} < 0.001$. N = 3 rats per group; n = 50 dendrites per rat.

3.4. COHORT 2. GluN1 distribution in CA3 dendrites from CIS rats following Oxy CPP

3.4.1. Following CIS, Oxy-males had elevated GluN1 in all cellular compartments of CA3 dendrites

Representative electron micrographs showing GluN1-SIG labeling in CA3 pyramidal cell dendrites for all four CIS groups are shown in Fig. 6A–D. Two-way ANOVA showed significant main effects of condition (Sal vs Oxy) on GluN1-SIG particle density on the plasma membrane ($F_{3,596} = 5.57$; $p = 0.008$), near the plasma membrane ($F_{3,596} = 3.31$; $p = 0.005$), in the cytoplasm ($F_{3,596} = 17.08$; $p < 0.0001$), and in total ($F_{3,596} = 31.47$; $p < 0.0001$) in CA3 dendrites from CIS rats. There was a significant interaction between sex and condition on GluN1-SIG particle density in the cytoplasm ($F_{3,596} = 17.08$; $p < 0.0001$) as well as in total ($F_{3,596} = 31.47$; $p < 0.0001$) of CA3 dendrites. Post hoc analysis revealed that CIS Sal-females compared to CIS Sal-males had significantly higher GluN1-SIG particle density in the cytoplasm ($p = 0.002$) and in total ($p = 0.01$) in CA3 dendrites (Fig. 7A and B). CIS Oxy-males compared to CIS Sal-males had significantly higher dendritic GluN1-SIG particle density on the plasma membrane ($p = 0.009$), near the plasma

membrane ($p = 0.02$), in the cytoplasm ($p < 0.0001$), and in total ($p < 0.0001$) (Fig. 7B). Moreover, CIS Oxy-males compared to CIS Oxy-females had significantly higher GluN1-SIG particle density on the plasma membrane ($p = 0.01$), in the cytoplasm ($p = 0.02$), and in total ($p < 0.0001$) in dendrites (Fig. 7A and B). There were no differences in the dendritic density of GluN1-SIG particles in CIS Sal-females compared to CIS Oxy-females in any cellular compartment.

Two-way ANOVA showed a significant main effect of sex on the partitioning ratios of GluN1-SIG particles on the plasma membrane ($F_{3,596} = 4.41$; $p = 0.002$) and in the cytoplasm ($F_{3,596} = 3.83$; $p = 0.0009$) in CA3 dendrites. Post hoc Tukey showed that CIS Oxy-females had a significantly lower ratio of GluN1-SIG particle on the plasma membrane compared to CIS Oxy-males ($p = 0.005$) (Fig. 7C and D). A post hoc Tukey showed that CIS Oxy-females had a significantly higher ratio of GluN1-SIG particles in the cytoplasm compared to CIS Oxy-males ($p = 0.03$) (Fig. 7C and D).

3.4.2. Following CIS, GluN1-containing spines increased in Oxy-males compared to Sal-males

The percent of GluN1-labeled spines as well as the subcellular

Fig. 6. Representative electron micrographs showing GluN1-SIG labeling in CA3 pyramidal cell dendrites for CIS Sal- and Oxy-female and male rats. **A-D.** Electron micrographs show the distribution of GluN1-SIG particles within CA3 pyramidal cell dendrites from CIS Sal-female (**A**), a CIS Sal-male (**B**), a CIS Oxy-female (**C**), and a CIS Oxy-male (**D**) rat. Examples of near plasmalemmal (triangle), on plasmalemmal (chevron), and cytoplasmic (arrow) GluN1-SIG particles in dendrites are shown. Scale bar: 500 nm.
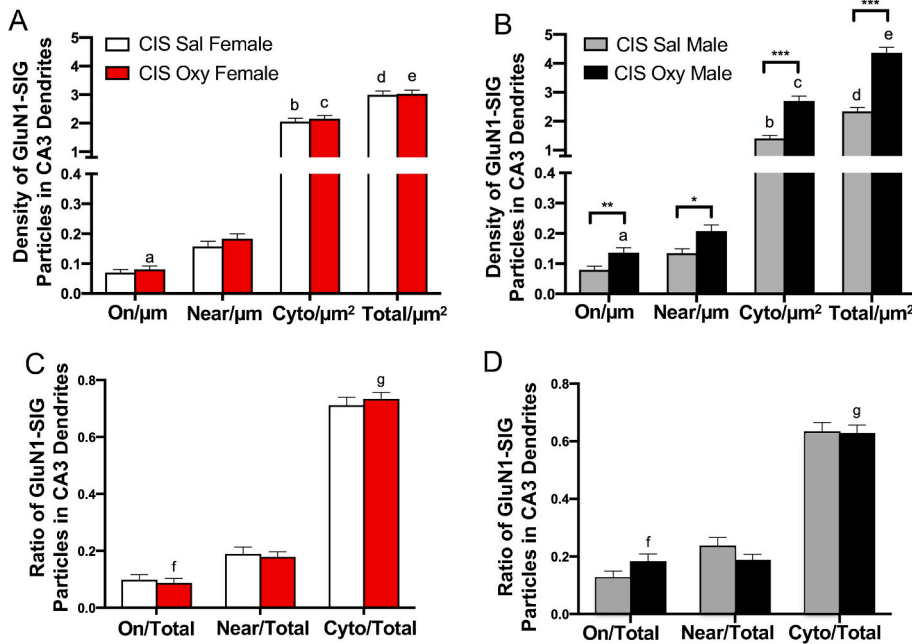
Fig. 7. Quantitative analysis of the distribution of GluN1-SIG particles in CA3 pyramidal cell dendrites in CIS Sal- and Oxy-female and male rats. **A, B.** CIS Sal-females compared to CIS Sal-males have a greater density of GluN1-SIG particles in the cytoplasm and in total in CA3 dendrites. In CIS females, there is no effect of Oxy CPP on the density of GluN1-SIG particles (**A**). However, CIS Oxy-males compared to CIS Sal-males (**B**) have a greater density of GluN1-SIG particles on and near the plasmalemma, in the cytoplasm, and in total in CA3 dendrites. CIS Oxy-females compared to CIS Oxy-males have a lower density of GluN1-SIG particles on the plasmalemma, in the cytoplasm, and in total in CA3 dendrites. **C, D.** CIS Oxy-females compared to CIS Oxy-males had a significantly lower ratio of GluN1-SIG particles on the plasma membrane, but a higher ratio of GluN1-SIG particles in the cytoplasm. ***$p < 0.001$, **$p < 0.01$, *$p < 0.05$, $p^f < 0.001$, $p^{a,b} < 0.01$, $p^{a,b,c,e,g} < 0.05$. N = 3 rats per group; n = 50 dendrites per rat.

distribution of GluN1 in spines in both SR and SLu was not different between CIS Sal- and Oxy-females (Table 1). However, in the SR, CIS Oxy-male rats had a higher percentage of GluN1 labeled spines compared to CIS Sal-males (*t*-test; p = 0.004), with most of the GluN1-SIG particles increasing in the cytoplasm (*t*-test; p = 0.004) (Table 1). Moreover, CIS Oxy-males compared to CIS Sal-males had significantly more (p = 0.043) GluN1-SIG particles at the synapse of SLu spines (Table 1).

In summary, baseline levels of GluN1 in CA3 dendrites remain elevated in females compared to males following CIS. However, CIS Oxy-females (which acquire Oxy CPP) compared to CIS Sal-females have

similar distributions of GluN1 in CA3 dendrites and spines. In contrast, CIS Oxy-males (which do not acquire Oxy CPP) compared to CIS Sal-males have increased densities of GluN1 in all cellular compartments of CA3 dendrites as well as in dendritic spines on both SR and SLu. Thus, these findings propose that CA3 dendrites and spines in CIS Oxy-males would have a greater capacity for glutamate binding of GluN1.
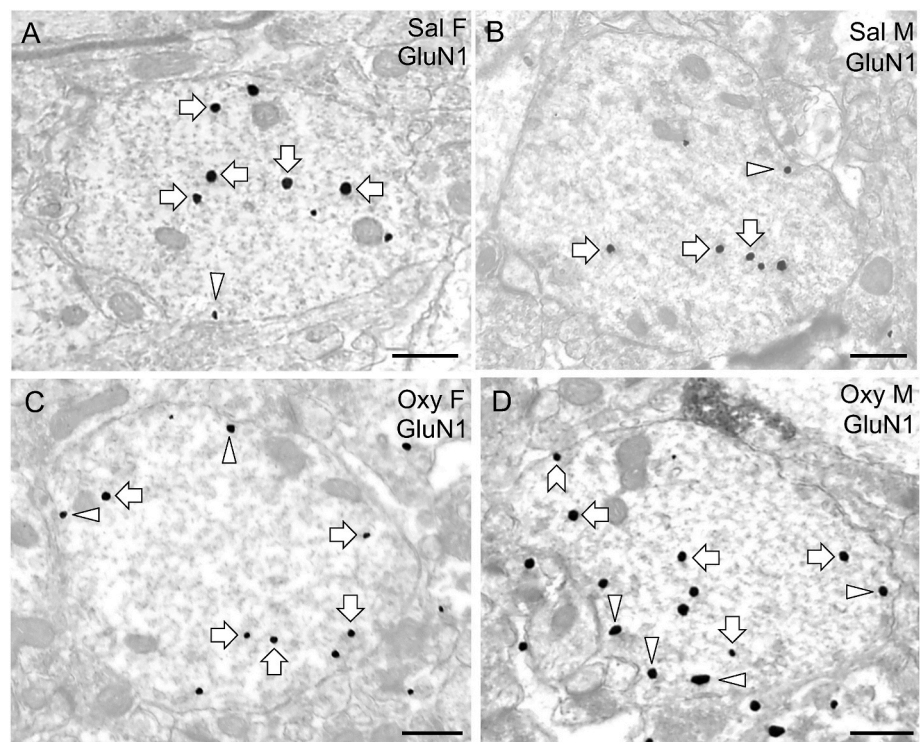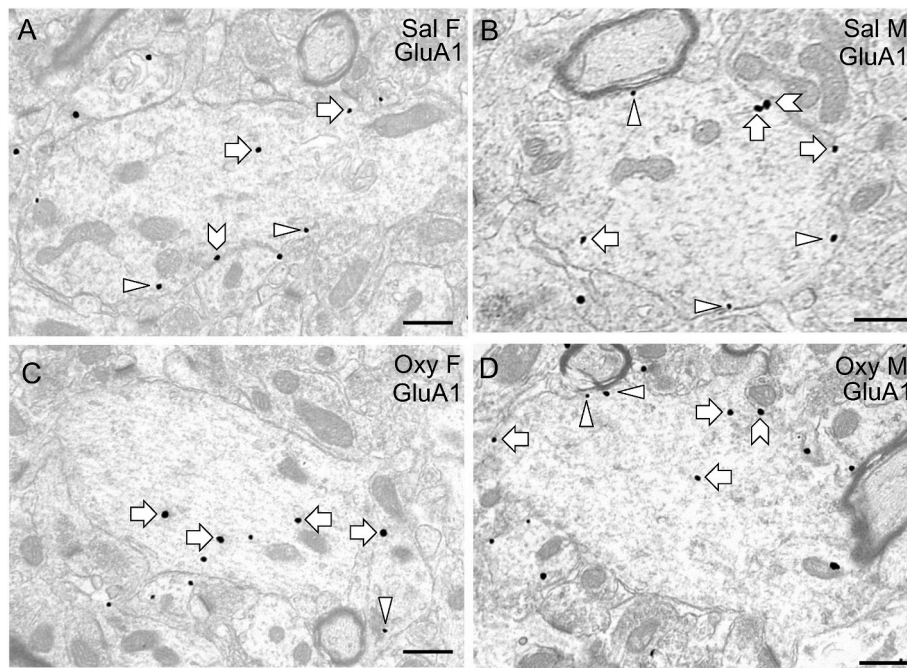

Fig. 8. Representative electron micrographs of GluA1-SIG particles in CA3 pyramidal cell dendrites in naïve Sal- and Oxy-female and male rats. **A-D.** Electron micrographs show the distribution of GluA1-SIG particles within dendrites from a Sal-female (**A**), a Sal-male (**B**), an Oxy-female (**C**), and an Oxy-male (**D**) rat. Examples of near plasmalemmal (triangle) and cytoplasmic (arrow) GluA1-SIG particles in dendrites are shown. Scale bar = 500 nm.

4. GluA1 results

4.1. COHORT 1. Following Oxy CPP, GluA1 redistributed from the near plasma membrane to the cytoplasm in large CA3 dendrites in females

4.1.1. Oxy-males had more GluA1-SIG particles near the plasma membrane

Representative electron micrographs showing GluA1-SIG labeling in CA3 pyramidal cell dendrites in SR for all four groups are shown in Fig. 8. GluA1-SIG particles were found on the plasma membrane, near the plasma membrane and in the cytoplasm of CA3 dendrites. There were no significant differences in the density of GluA1-SIG particles in the plasma membrane, cytoplasm or in total in CA3 dendrites between any of the four groups of unstressed rats (Fig. 9A and B). When the GluA1-containing dendrites were divided by size (i.e., large vs small), there was no difference in the density of GluA1 in any cellular compartment in the four groups (not shown).

There also were no differences in the partitioning ratios of GluA1 in any cellular compartment when examining CA3 dendrites of all sizes (Fig. 9C and D). However, two-way ANOVA of the ratio of cytoplasmic GluA1-SIG particles in large CA3 dendrites revealed a main effect of sex ($F_{3,245} = 4.39$; $p = 0.02$) and treatment ($F_{3,245} = 4.39$; $p = 0.02$), as well as an interaction verging on significance between treatment and sex ($F_{3,245} = 4.39$; $p = 0.06$). Two-way ANOVA also showed that the ratio of GluA1-SIG particles near the plasma membrane of large dendrites had a trending interaction of sex and treatment ($F_{3,245} = 2.67$; $p = 0.06$). Post hoc Tukey in large CA3 dendrites showed that US Oxy-females compared to Sal-females had a significantly greater ratio of GluA1-SIG particles in the cytoplasm ($p = 0.02$) (Fig. 9E). Moreover, Oxy-females

compared to Oxy-males had a lower ratio ($p = 0.05$) of GluA1-SIG particles near the plasma membrane but a greater ratio ($p = 0.02$) of GluA1-SIG particles in the cytoplasm in large CA3 dendrites (Fig. 9E and F).

4.2. Oxy CPP had few effects on GluA1 distributions in CA3 spines in females or males

Representative examples of GluA1 labeled spines in the SR and SLu are shown in Fig. 10. These were no differences in the percentage GluA1 labeled spines in either the SR or SLu in any of the four groups. However, in the SR, Sal-females compared to Sal-males tended to have more GluA1 particles localized to the membrane ($p = 0.06$) of dendritic spines (Table 2). In the SLu, Sal-females compared to Sal-males tended to have more GluA1 labeling at the synapse ($p = 0.078$) of dendritic spines (Table 2). Sal-females compared to Oxy-females had a significantly higher percentage of GluA1 particles ($p = 0.02$) in the cytoplasm of SLu spines contacted by mossy fibers (Table 2). In contrast, Oxy-males compared to Sal-males had greater GluA1 particles in the cytoplasm ($p = 0.009$) of SLu spines contacted by mossy fibers (Table 2).

In summary, there were no baseline differences in the density of GluA1 in CA3 dendrites between females and males. However, Sal-females compared to Sal-males had more GluA1 on mossy fiber CA3 synapses. Moreover, although Oxy CPP had few effects on GluA1 densities in CA3 dendrites in sex, GluA1 in Oxy-females compared to Sal-females near the plasmalemma redistributed to the cytoplasm of CA3 dendrites suggesting reduced pools of GluA1 available for ligand binding.
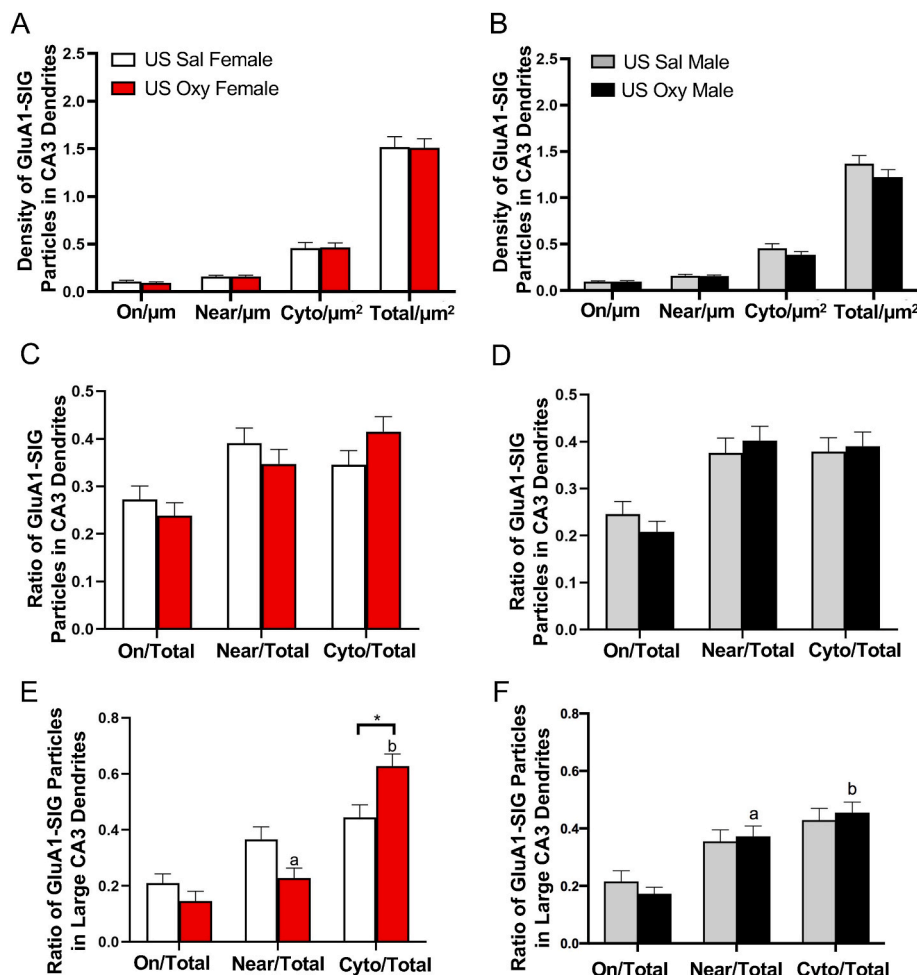
Fig. 9. Quantitative analysis of the distribution of GluA1-SIG particles in CA3 pyramidal cell dendrites in naïve Sal- and Oxy-female and male rats. **A-B** There were no observed within or across sex differences in the distribution of GluA1-SIG particles in CA3 pyramidal cell dendrites. **C, D.** There were no observed within or across sex differences in the partitioning ratios of GluA1 in any cellular compartment of CA3 pyramidal cell dendrites. **E, F.** When specifically selecting for large dendrites, treatment and sex differences were revealed. US Oxy-females compared to US Sal-females had a significantly greater ratio of GluA1-SIG particles in the cytoplasm of large CA3 dendrites. Moreover, US Oxy-males compared to US Oxy-females have a greater ratio of GluA1-SIG particles near the cytoplasm, but a smaller ratio of GluA1-SIG particles in the cytoplasm., $*p < 0.05$, $p^a = 0.05$, $p^b < 0.05$. N = 3 rats per group; n = 50 dendrites per rat.
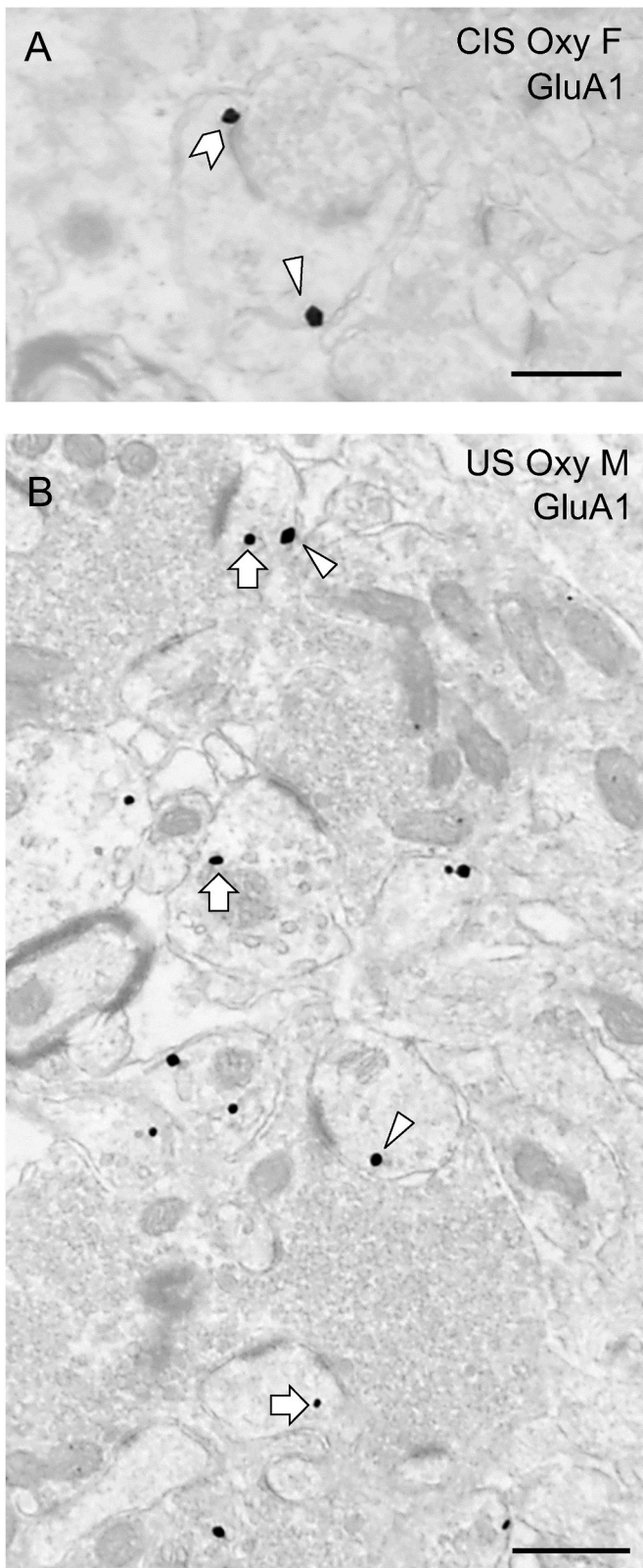
Fig. 10. Examples of GluA1-labeled spines in CA3. Usually one GluA1-SIG particle was found in a single dendritic CA3 spine, but sometimes more than one was detected. **A.** A SR spine of a CIS Oxy-male has GluA1-SIG particles on the synapse (chevron) and near the plasma membrane (arrowhead). **B.** Numerous dendritic spines containing GluA1-SIG particles and contacted by mossy fibers are observed in SLu. Examples of near plasma membrane (arrowhead) and cytoplasmic (arrows) GluA1-SIG particles are shown. Scale bar: 500 nm.

4.3. COHORTS 1 & 2. GluA1 distribution in CA3 dendrites from Sal naïve compared to CIS rats

4.3.1. CIS elevates GluA1 in CA3 dendrites and mossy fiber synapses in males

There were no significant differences in naïve (US) vs CIS saline rats when comparing GluA1 distribution in all CA3 dendrites. However, when separated by size, CIS males had more GluA1-SIG particles in small CA3 dendrites than the other three groups (Fig. 11A and B). Two-way ANOVA of small dendrites revealed a significant main effect of treatment on the density of GluA1-SIG particles on the plasma membrane ($F_{3,353} = 3.12$; $p = 0.006$) and interaction between sex and treatment on GluA1-SIG density in total ($F_{3,353} = 2.52$; $p = 0.02$). Post hoc Tukey showed that CIS males compared to US males tended to have a greater density of GluA1-SIG particles on the plasma membrane that trended toward significance ($p = 0.06$) and a significantly greater density of GluA1-SIG particles in total ($p = 0.04$) in small CA3 dendrites (Fig. 11B). Two-way ANOVA showed a significant main effect of treatment ($F_{3,353} = 2.28$; $p = 0.03$) on the ratio of GluA1 in the cytoplasm of small CA3 dendrites. Post hoc analysis showed that the ratio of GluA1-SIG particles in the cytoplasm of small CA3 dendrites tended to be greater ($p = 0.06$) in US males than CIS males (Fig. 11D). There were no significant differences between US and CIS Sal-female rats in either the density or ratio of GluA1 in small dendrites (Fig. 11A,C).

4.4. CIS increased GluA1 synaptic labeling in CA3 spines in males

There were no differences in the percentage of GluA1 labeled spines in either the SR or SLu in females and males. However, CIS Sal-males compared to US Sal-males tended to have a greater ($p = 0.065$) number of GluA1-SIG particles on the synapse of SR spines (Table 2). Similarly CIS Sal-males compared to US Sal-males had significantly more GluA1 particles at the synapse ($p = 0.0002$) and in the cytoplasm ($p = 0.05$) of spines contacted by mossy fibers in SLu (Table 2).

<u>In summary</u>, CIS does not alter the baseline distributions of GluA1 in CA3 dendrites and spines in females. In contrast, CIS increases GluA1 on the plasma membrane and in total in small CA3 dendrites and in the synapse of dendritic spines in males.

4.5. COHORT 2. GluA1 distribution in CA3 dendrites from CIS rats following Oxy CPP

4.5.1. Oxy-males had more GluA1-SIG particles in total and in the cytoplasm

Representative electron micrographs showing GluA1-SIG labeling in CA3 pyramidal cell dendrites for all four CIS groups are shown in Fig. 12. There were no significant differences between any of the groups in the density of GluA1 in all CA3 dendrites. However, when the dendrites were further subdivided by size, group differences in the density of GluA1 emerged. Two-way ANOVA of large dendrites showed a main effect of sex ($F_{3,218} = 7.40$; $p = 0.04$), treatment ($F_{3,218} = 7.39$; $p = 0.01$), and interaction between sex and treatment ($F_{3,218} = 7.40$; $p = 0.0003$) for the density of GluA1-SIG particles in the cytoplasm of CIS rats. Tukey post hoc showed that CIS Oxy-males exhibit greater GluA1-SIG particle density in the cytoplasm of large CA3 dendrites compared to CIS Sal-males ($p < 0.0001$; Fig. 13B) and Oxy-females ($p = 0.0003$; Fig. 13A). Two-way ANOVA of large dendrites revealed a main effect of sex ($F_{3,218} = 9.17$; $p = 0.02$), treatment ($F_{3,218} = 9.17$; $p < 0.0001$), and interaction between sex and treatment ($F_{3,218} = 9.17$; $p < 0.0001$) for the density of GluA1-SIG particles in total for CIS rats. Tukey HSD showed that CIS Oxy-males exhibit greater GluA1-SIG particle density in large dendrites in total compared to both CIS Sal-males ($p < 0.0001$) and CIS Oxy-females ($p = 0.0006$) (Fig. 13A and B).

Two-way ANOVA of all dendrites revealed a main effect of treatment (Sal vs Oxy) [$F_{3, 596} = 2.23$; $p = 0.05$] for the ratio of plasma membrane GluA1-SIG particles for CIS rats. Post hoc Tukey showed CIS Oxy-
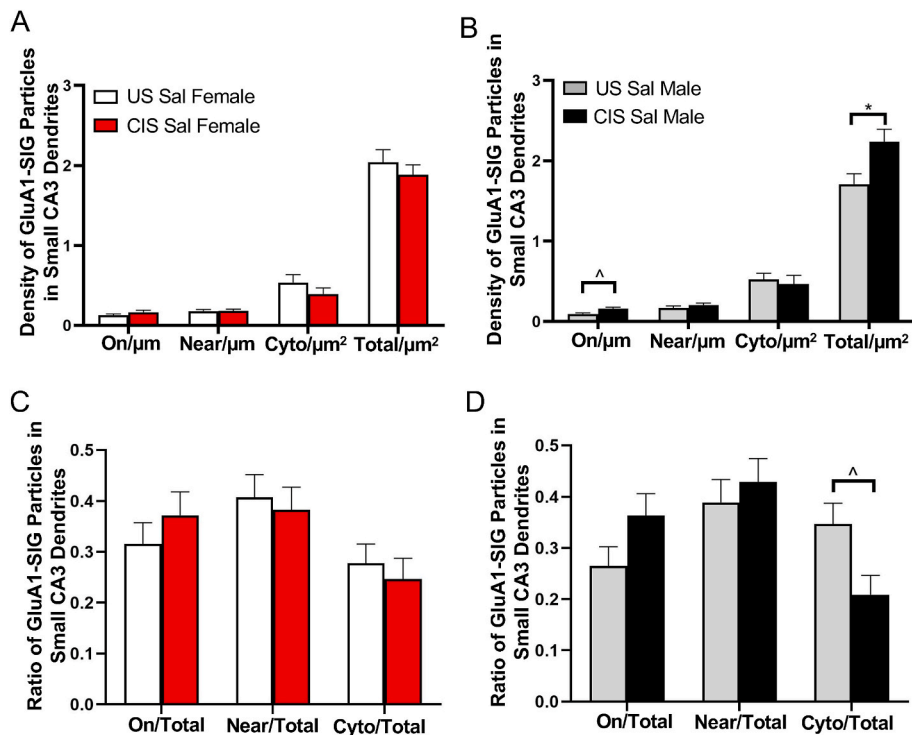
Fig. 11. Quantitative analysis of the distribution of GluA1-SIG particles in small CA3 pyramidal cell dendrites in unstressed (US) and CIS Sal-female and Sal-male rats. **A-D.** There are no sex differences between US or CIS Sal-female or Sal-male rats when comparing density or partitioning ratio of GluA1-SIG particles in small CA3 dendrites. Furthermore, there are no differences observed between US and CIS Sal-female rats for density **(A)** and portioning ratio **(C)** of GluA1-SIG particles in small CA3 dendrites. There are, however, significant differences between US Sal-male and CIS Sal-male rats in GluA1-SIG particles density **(B)** and partitioning ratio **(D)** in small CA3 dendrites. **B.** CIS males compared to US males had greater density of GluA1-SIG particles on the plasma membrane and in total in small CA3 dendrites. **D.** Moreover, the ratio of GluA1-SIG particles in the cytoplasm of small CA3 dendrites was greater in US males than CIS males. *p < 0.05, ^p = 0.06. N = 3 rats per group; n = 50 dendrites per rat.

females tended to have a (p = 0.06) greater ratio of GluA1-SIG particles on the plasma membrane of all CA3 dendrites compared to Sal-females, which verged on significance (Fig. 13C). There were no differences in the ratio of GluA1 in any cellular compartment in CA3 dendrites in males (Fig. 13D).

When divided by dendritic size, additional differences in GluA1 distributions emerged. Two-way ANOVA of large dendrites revealed a significant interaction between sex and treatment ($F_{3, 218} = 2.52$; p = 0.04) for the ratio of GluA1-SIG particles in the cytoplasm of CIS rats. Tukey post hoc showed CIS Sal-females compared to Oxy-females exhibited a greater ratio of GluA1-SIG particles in the cytoplasm (p = 0.04) of large dendrites (Fig. 13E). There were no differences in the ratio of GluA1 in any cellular compartment in large CA3 dendrites in males (Fig. 13F).

4.6. CIS males have elevated GluA1 in CA3 dendritic spines

The percentage of GluA1 dendritic spines in SR is greater and trended towards significance in CIS Sal-males compared to CIS Sal-females (p = 0.07) (Table 2). There are no differences in the percentage of GluA1 spines contacted by mossy fibers in CA3 spines in any group. However, the number of GluA1 labeled mossy fiber SLu synapses is higher in CIS Sal-males compared to CIS Sal-females (p = 0.05) (Table 2).

<u>In summary</u>, at baseline CIS males have higher percentages of GluA1 containing CA3 dendritic spines compared to CIS females. In CIS females, Oxy CPP elevates the proportion of GluA1 on the plasma membrane of CA3 dendrites. In contrast, CIS Oxy-males (which do not acquire Oxy CPP) results in an elevation of cytoplasmic GluA1 in large CA3 dendrites as well as an increase in synaptic GluA1 in SR spines. These results propose that Oxy exposure would alter the sensitivity of different portions of CA3 dendrites to ligand binding in females and males.

4.7. COHORTS 1 & 2. GluA1 distribution in CA3 dendrites from Oxy naïve vs CIS Oxy rats

4.7.1. CIS Oxy-male and female rats had greater densities GluA1 in CA3 dendrites compared to US Oxy rats

Two-way ANOVA of all dendrites revealed a main effect of condition ($F_{3,596} = 6.20$; p < 0.0001) for the density of GluA1-SIG particles on the plasma membrane in Oxy rats. Tukey post hoc showed that CIS Oxy-females compared to US Oxy-females exhibit greater GluA1-SIG particle density on the plasma membrane (p = 0.005; Fig. 14A). Similarly, CIS Oxy-males compared to US Oxy-males exhibit greater GluA1-SIG particle density on the plasma membrane (p = 0.04; Fig. 14B). Two-way ANOVA of all dendrites also showed a main effect of condition ($F_{3,596} = 5.87$; p = 0.002) and interaction between treatment and condition ($F_{3,596} = 5.87$; p = 0.005) for the density of GluA1-SIG particles in total in Oxy rats. Tukey post hoc showed a greater dendritic density of GluA1-SIG particles in total in CA3 dendrites in CIS males compared to US males (p = 0.0002; Fig. 14B).

Next, the density of GluA1 in CA3 dendrites of different sizes was analyzed in the four groups. Two-way ANOVA of large dendrites revealed a main effect of condition ($F_{3,224} = 4.09$; p = 0.0007) for the density of GluA1-SIG particles on the plasma membrane in Oxy rats. Tukey post hoc showed that plasma membrane GluA1-SIG particle density increased in CIS Oxy-females (p = 0.05) compared to their unstressed Oxy cohorts (Fig. 14C).

Two-way ANOVA of large dendrites showed a main effect of sex approaching significance ($F_{3,224} = 5.81$; p = 0.06) and a significant interaction between treatment and condition ($F_{3,224} = 5.81$; p < 0.0001) for the density of GluA1-SIG particles in the cytoplasm in Oxy rats. Tukey HSD showed that CIS Oxy-males had greater GluA1-SIG particle density in the cytoplasm of large CA3 dendrites compared to CIS Oxy-females (p = 0.001). Similarly, CIS Oxy-males exhibit greater GluA1-SIG particle density in the cytoplasm (p = 0.005) compared to US Oxy-males (Fig. 14D). Two-way ANOVA of large dendrites revealed a main effect of sex ($F_{3,224} = 6.97$; p = 0.004), condition ($F_{3,224} = 6.97$; p = 0.001), and interaction between treatment and condition ($F_{3,224} = 6.97$; p = 0.003) for the density of GluA1-SIG particles in total in Oxy

Table 2
GluA1-labeled spines in CA3.

Group	% ± SEM labeled spines	Location[a]		
		synapse	membrane	cytoplasm
SR				
Male Sal	11.67 ± 2.33	**0.67 ± 0.30[a]**	**1.0 ± 0.58[b]**	10.0 ± 2.65
Male Oxy	10.33 ± 0.88	0.67 ± 0.33	3.0 ± 1.53	7.33 ± 1.20
Female Sal	11.0 ± 2.89	0.33 ± 0.30	**5.0 ± 1.53[b]**	7.0 ± 3.0
Female Oxy	10.33 ± 3.28	0.33 ± 0.33	2.33 ± 1.33	9.0 ± 3.46
SLu				
Male Sal	16.0 ± 2.52	**0.33 ± 0.33[c,d]**	15.0 ± 2.52	**4.33 ± 1.67[e,f]**
Male Oxy	17.67 ± 4.70	**0.0 ± 0.0[g]**	8.33 ± 4.33	**13.0 ± 2.08[e]**
Female Sal	12.33 ± 4.48	**2.67 ± 1.33[c]**	9.0 ± 3.0	**9.0 ± 1.0[h]**
Female Oxy	12.0 ± 4.16	**2.33 ± 0.88[g]**	7.33 ± 2.91	**5.33 ± 2.19[h]**
CIS SR				
Male Sal	**18 ± 3.21[i]**	**2.33 ± 0.88[a]**	9.0 ± 5.29	8.33 ± 2.03
Male Oxy	15 ± 4.16	2.67 ± 1.20	4.33 ± 2.19	8.0 ± 1.53
Female Sal	**10.33 ± 1.33[i]**	1.0 ± 0.58	5.67 ± 1.86	5.0 ± 1.53
Female Oxy	14 ± 5.13	2.0 ± 1.53	7.0 ± 2.65	5.0 ± 1.53
CIS SLu				
Male Sal	26.33 ± 4.06	**8.0 ± 0.58[j,d]**	11.67 ± 3.38	**10.67 ± 2.33[f]**
Male Oxy	24.0 ± 4.58	3.0 ± 1.53	9.67 ± 2.91	12.33 ± 1.33
Female Sal	21.33 ± 4.84	**1.33 ± 0.88[j]**	13.33 ± 2.03	7.0 ± 2.31
Female Oxy	25.33 ± 7.80	5.33 ± 3.53	16.67 ± 5.55	8.33 ± 0.67

a: ^p = 0.0755. b: ^p = 0.0615. c: ^p = 0.0780. d: ***p = 0.0002. e: **p = 0.0092. f: *p = 0.0469. g: ^p = 0.0780. h: *p = 0.0166. i: ^p = 0.0657. j: *p = 0.0456.

[a] Some spines had more than one GLUA1-SIG particle.

rats. Tukey post hoc showed that CIS Oxy-males exhibit greater GluA1-SIG particle density in total (p = 0.0008) compared to CIS Oxy-females. Similarly, CIS Oxy-males had greater GluA1-SIG particle density in total compared to US Oxy-males (p = 0.0002; Fig. 14D).

5. GluA1 redistributes to the plasma membrane of CA3 dendrites in CIS Oxy-females and males

Two-way ANOVA showed significant main effects of condition (US vs CIS) on the ratio of GluA1-SIG particles on the plasma membrane ($F_{3,596}$ = 9.15; p < 0.0001) and in the cytoplasm ($F_{3,596}$ = 4.17; p = 0.006) of CA3 dendrites in Oxy rats. Tukey post hoc showed a greater ratio of GluA1-SIG particles on the plasma membrane in CIS Oxy-females compared to US Oxy-females (p = 0.0004) as well as in CIS Oxy-males compared to US Oxy-males (p = 0.02; Fig. 14E and F). There also was a greater ratio of GluA1-SIG particles in the cytoplasm in US Oxy-females compared to CIS Oxy-females (p = 0.02; Fig. 14E).

When the ratio of GluA1 was analyzed in CA3 dendrites of different sizes, additional differences were found. Two-way ANOVA of large dendrites showed a main effect of condition ($F_{3,224}$ = 3.85; p = 0.008) for the ratio of GluA1-SIG particles on the plasma membrane in Oxy rats. Tukey post hoc showed CIS Oxy-females exhibited a greater ratio of GluA1-SIG particles on the plasma membrane in large dendrites compared to US Oxy-females (p = 0.01; Fig. 14G). Two-way ANOVA of large dendrites showed an interaction between treatment and condition ($F_{3,224}$ = 2.24; p = 0.04) for the ratio of GluA1-SIG particles near the plasma membrane. Tukey post hoc showed US Oxy-males compared to US-females had a greater ratio verging on significance (p = 0.06) of GluA1-SIG particles near the plasma membrane of large dendrites (Fig. 14G). Two-way ANOVA of large dendrites revealed a main effect of condition ($F_{3,224}$ = 6.50; p = 0.008) as an interaction between treatment and condition ($F_{3,224}$ = 6.50; p = 0.001) for the ratio of GluA1-SIG particles in the cytoplasm. Post hoc showed US Oxy-females exhibited a greater ratio of GluA1-SIG particles in the cytoplasm of large dendrites compared to CIS Oxy-females (p = 0.0001; Fig. 14G). US Oxy-females had a greater GluA1-SIG particle ratio in the cytoplasm compared to US Oxy-males (p = 0.02; Fig. 14G and H).

The percentage of GluA1 labeled spines as well as the subcellular distribution of GluA1 in dendritic spines in both SR and SLu was similar in all four Oxy groups (Table 2).

In summary, regardless of differences in CPP responses, CIS
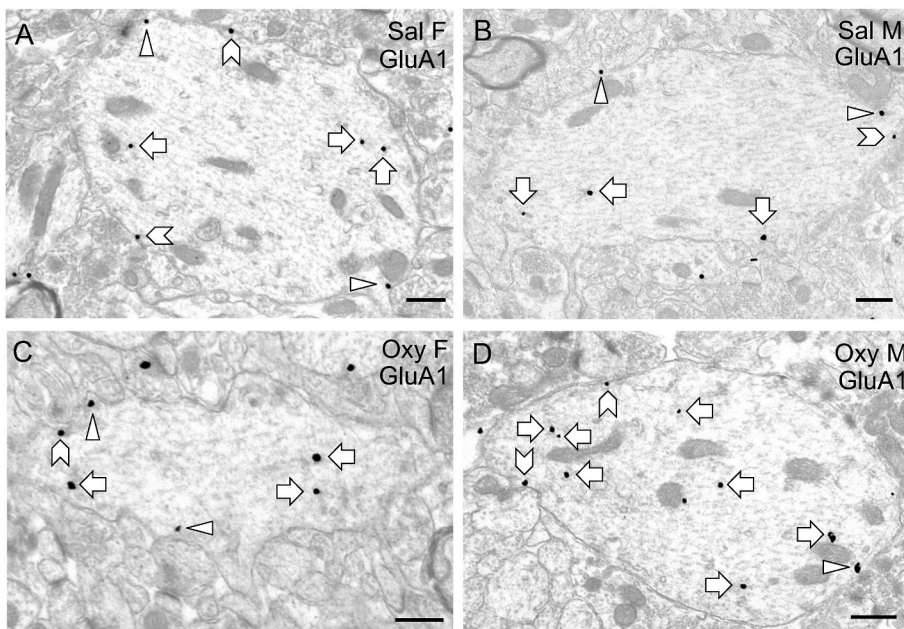
Fig. 12. Representative electron micrographs showing GluA1-SIG labeling in CA3 pyramidal cell dendrites for CIS Sal- and Oxy-female and male rats. **A-D.** Electron micrographs show the distribution of GluA1-SIG particles within CA3 pyramidal cell dendrites from a CIS Sal-female **(A),** a CIS Sal-male **(B),** a CIS Oxy-female **(C),** and a CIS Oxy-male **(D)** rat. Examples of near plasmalemmal (triangle), on plasmalemmal (chevron), and cytoplasmic (arrow) GluN1-SIG particles in dendrites are shown. Scale bar: 500 nm.
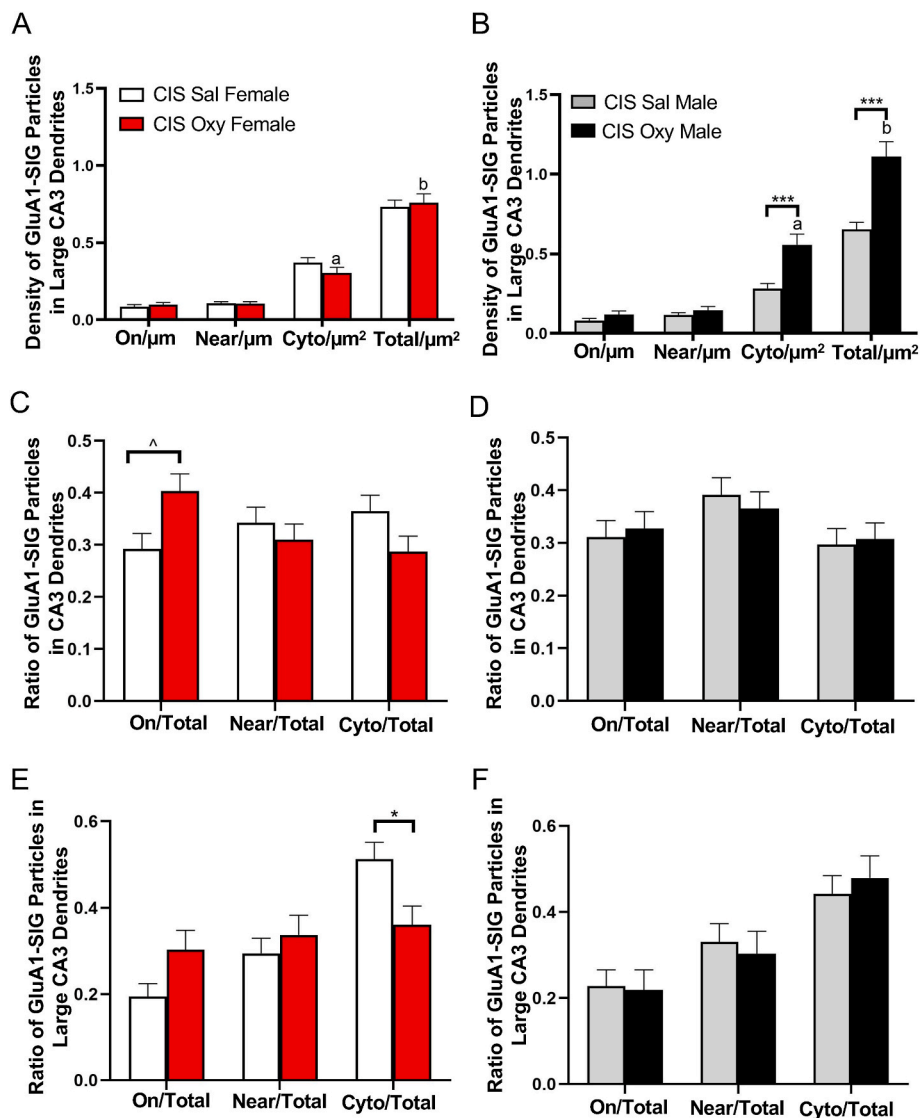
Fig. 13. Quantitative analysis of the distribution of GluA1-SIG particles in CA3 pyramidal cell dendrites in CIS Sal- and Oxy-female and male rats. **A, B.** There were no sex differences between CIS Sal-female and Sal-male rats. However, there were significant differences between CIS Oxy-female and CIS Oxy-male rats, with CIS-male rats demonstrating greater density of GluA1-SIG particles in the cytoplasm and in total in large CA3 dendrites. Moreover, while there were no treatment differences between CIS Oxy- and Sal-female rats (**A**), there were differences observed between CIS Oxy- and Sal-male rats. CIS Oxy-male rates compared to CIS Sal-male rates had a greater density of GluA1-SIG particles in the cytoplasm and in total in large CA3 dendrites (**B**). **C–F.** There were no significant sex differences between CIS Sal- or Oxy-female or male rats in the partitioning ratio of GluA1-SIG particles in CA3 of all sizes or specifically in large CA3 dendrites. However, there were significant treatment differences specifically between CIS Sal- and Oxy-female, not male (**D, F**), rats in the partitioning ratio of GluA1-SIG particles in both CA3 dendrites of all sizes (**C**) and large CA3 dendrites (**E**). CIS Oxy-females as opposed to CIS Sal-females had a greater ratio of GluA1-SIG particles on the plasmalemma across CA3 dendrites of all sizes. When specifically examining large CA3 dendrites, CIS Oxy-females as compared to CIS Sal-females had a decreased ratio of GluA1-SIG particles in the cytoplasm. ***$p < 0.001$, *$p < 0.05$, ^$p = 0.06$, $p^{a,b} < 0.001$. N = 3 rats per group; n = 50 dendrites per rat.

increased GluA1 on the plasma membrane of Oxy-females and Oxy-males. These findings suggest that CIS combined with behavior increases the availability of GluA1 for ligand binding on CA3 pyramidal cell dendrites in both females and males.

6. Discussion

Our EM studies reveal that females compared to males have elevated baseline levels of GluN1, but not GluA1, in CA3 pyramidal cell dendrites in both unstressed and CIS conditions. Moreover, following Oxy CPP, pools of GluN1 available for ligand binding decrease in CA3 dendrites of unstressed females so that they are similar to baseline levels seen in males. Following CIS, Oxy-males (which did not acquire CPP) had increased GluN1 and GluA1 in most subcellular compartments of CA3 pyramidal dendrites, signifying increased pools of glutamate receptors available for ligand binding. Together with our prior experiments, the upregulation of GluN1 and GluA1 following CIS in males may contribute to an increased sensitivity of CA3 neurons to glutamate and reduced capacity to redistribute other receptors and signaling molecules within CA3 pyramidal neurons important for Oxy CPP responses.

7. Methodological considerations

The present study has continued the work we performed over the last decade to not only elucidate how the hippocampal opioid system varies with sex, but also to determine the relationship of stress conditions and drug-related learning [reviewed in (McEwen and Milner, 2017; Chalangal et al., 2021)]. As constant estrous cycling monitoring could interfere with Oxy CPP behaviors (Walker et al., 2001, 2002; Van Kempen et al., 2014), estrous cycle phase was determined only after the rats were anesthetized on the day of euthanasia. Vaginal smear cytology was used to ensure all female rats used in the final experiments were in the estrus phase of the estrous cycle (Ryan et al., 2018; Reich et al., 2019). We acknowledge that a single measure of vaginal cytology cannot determine the stage of estrous cycle with absolute certainty. However, as our prior studies have extensively examined the effect of estrous phase cycle on the trafficking of opioid receptors in hippocampal neurons in unstressed and stressed rats [reviewed in (Chalangal et al., 2021)], it was not necessary to repeat this analysis in the current study. Additionally, the rats in each cohort were handled by the same experimenters for both the CPP behavior and CIS procedure to minimize experimental variability. Behavior procedures and euthanasia was performed on each cohort of male and female rats at the same time of the day. The current study used CA3 hippocampal tissue from different
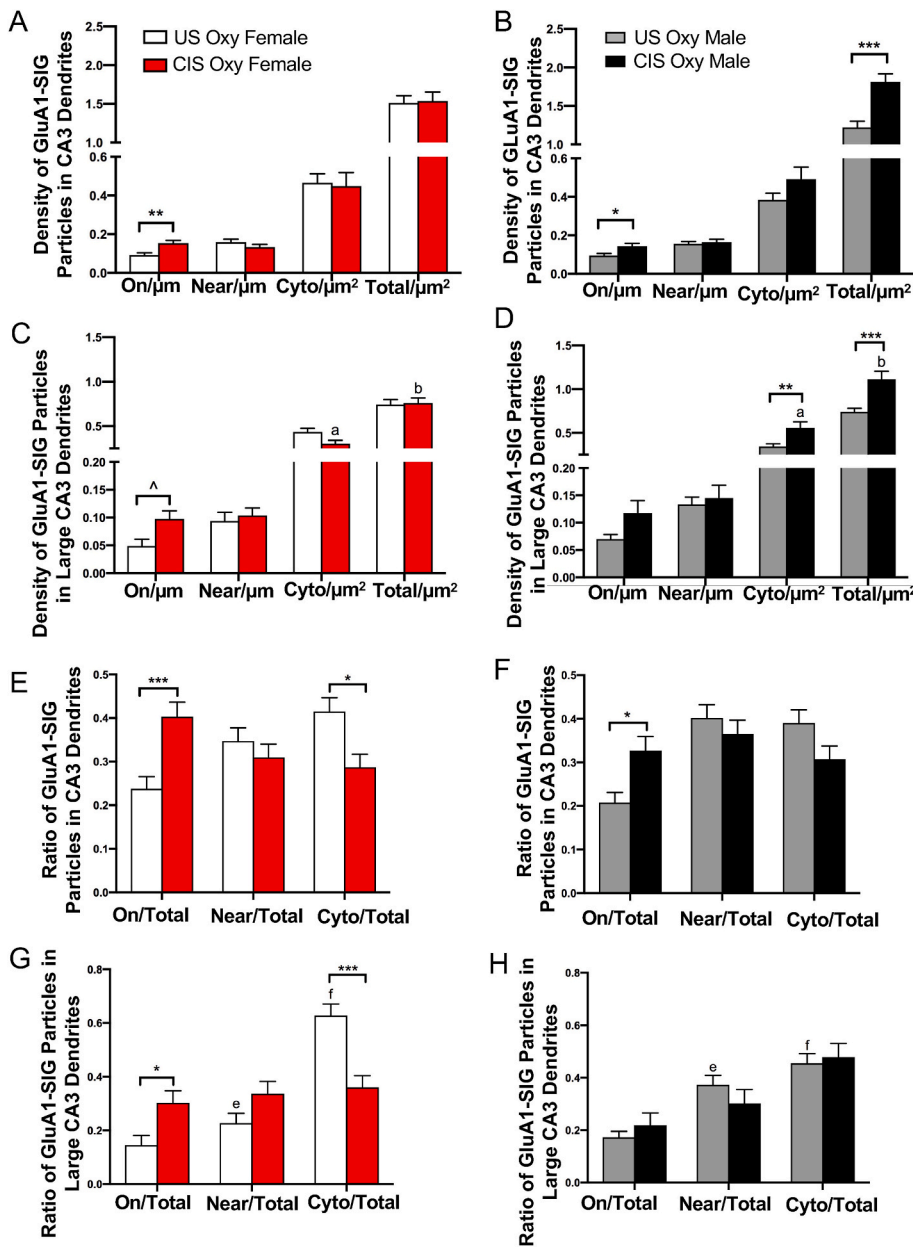
Fig. 14. Quantitative analysis of the distribution of GluA1-SIG particles in CA3 pyramidal dendrites in unstressed (US) and CIS Oxy-female and Oxy-male rats. **A-D.** There were no observed sex differences between US Oxy-female and Oxy-male in the density of GluA1-SIG particles in CA3 dendrites of all sizes or specifically within large CA3 dendrites. After undergoing CIS Oxy-females had a greater density of GluA1-SIG particles on the plasmalemma in CA3 dendrites of all sizes and specifically in large CA3 dendrites **(A, C)**. After undergoing CIS Oxy-males had a greater density of GluA1-SIG particles on the plasmalemma and in total in CA3 dendrites of all sizes, and a greater density of GluA1-SIG particles on the plasmalemma, in the cytoplasm, and in total in large CA3 dendrites **(B, D)**. When examining partitioning ratios, CIS Oxy-females compared to US Oxy-females had a greater ratio of GluA1-SIG particles on the plasmalemma in large CA3 dendrites and CA3 dendrites of all sizes, but a decreased ratio of GluA1-SIG particles in the cytoplasm of large CA3 dendrites and CA3 dendrites of all sizes. CIS Oxy-males as compared to US Oxy-males had an increased ratio of GluA1-SIG particles on the plasmalemma of CA3 dendrites of all sizes **(F)**, but no observed differences in partitioning ratios in large CA3 dendrites **(H)**. **A-B.** CIS Oxy-males as compared to CIS Oxy-females had a greater density of GluA1-SIG particles in the cytoplasm and in total in CA3 dendrites of all sizes and in large CA3 dendrites. However, US Oxy-female rats compared to US Oxy-male rats have a decreased ratio of GluA1-SIG particles near the plasmalemma and a greater ratio of GluA1-SIG particles in the cytoplasm specifically in large CA3 dendrites **(G–H)**, an effect which is not observed when examining CA3 dendrites of all sizes **(E–F)**. ***p < 0.001,**p < 0.01, *p < 0.05, ˆp < 0.06, p^b < 0.001, p^a < 0.01, p^c = 0.001, p^d = 0.008, p^f < 0.05, p^e = 0.06. N = 3 rats per group; n = 50 dendrites per rat.

cohorts (Ryan et al., 2018; Reich et al., 2019) that were processed simultaneously to allow for comparison between 8 groups of rats. We studied two glutamate receptor subunits, GluN1 and GluA1, in both cohort 1 and 2 rats. Cohort 1 consisted of unstressed Oxy CPP and unstressed saline males and females; cohort 2 consisted of CIS Oxy CPP and CIS saline males and females. This experimental set-up allowed us to observe the differences between GluN1 and GluA1 subunit distribution as related to differences in sex, CIS, and Oxy CPP behavior. We did not include saline- or Oxy-injected rats that did not undergo CPP training in the present study as our recent study demonstrated that these groups of rats had few changes in the redistribution of MORs and DORs in hippocampal neurons (Ashirova et al., 2021). We thus focused the current study on analyzing experimental groups which had previously shown changes in opioid receptor trafficking (Chalangal et al., 2021). Analyzing how CPP behavior may influence GluN1 and GluA1 subunit trafficking in hippocampal neurons in rats that do not undergo behavioral testing would be a subject of future study.

7.1. Baseline differences in glutamate receptor subunit distributions

We studied the baseline differences in glutamate receptor distributions of GluN1 and GluA1 subunits by comparing groups of unstressed male and female Sal-rats. Sal-females (which were in elevated estrogen states) had higher numbers of baseline cytoplasmic and total GluN1 subunits in CA3 dendrites as compared to Sal-males. As for GluA1 subunit density in CA3 dendrites, there was no baseline sex difference. Prior studies have found that elevated estrogen levels increase CA1 pyramidal cell synapse and spine densities (Gould et al., 1990) and enhance NMDA binding which is associated with improved working memory (Daniel and Dohanich, 2001). Moreover, others (Woolley et al., 1997) have demonstrated that increases in CA1 spine densities from administered estradiol in ovariectomized female rats are paralleled by an increase in NMDA receptor binding and sensitivity to NMDA receptor-mediated synaptic input, but not AMPA. While it is important to distinguish that we did not administer estradiol to rats, our data was similar in that female rats, with elevated estrogen levels at baseline, had greater GluN1 density in CA3 pyramidal cell dendrites than male rats but similar GluA1

subunit density.

It is widely known and accepted that NMDA receptors (containing GluN1) are directly involved in promoting both LTP (Bliss and Collingridge, 1993) and long-term depression (LTD) (Bear and Malenka, 1994). It has also been shown that mice lacking GluA1-containing AMPA receptors display impairment of LTP, demonstrating the importance of this glutamate receptor (Zamanillo et al., 1999). Specifically, it has been suggested that estradiol induces morphologic change of dendritic spine and synapses in the hippocampus to cause increased neuronal excitability (Woolley et al., 1997). Estrogen has effects on learning behaviors and memory function, and one theory of how elevated estrogen increases NMDA receptor binding in the CA1 is through acetylcholine binding at the M2 muscarinic receptor (Daniel and Dohanich, 2001). Furthermore, glutamate, the key substrate of both NMDA and AMPA receptors, plays an important role in the neurobiology of drug addiction including craving, relapse, and withdrawal (Tzschentke and Schmidt, 2003; Hou et al., 2009). Taken together, our finding that Sal-female rats have greater densities of GluN1 receptor subunits in CA3 dendrites may suggest a potential for heightened baseline glutamate sensitivity in the hippocampus of females and subsequently, an increased predisposition for the aforementioned effects of GluN1 transmission including LTP.

AMPA receptors are known to be essential for excitatory transmission and hippocampal synaptic plasticity as well (Barkóczi et al., 2012). Deficits in LTP and LTD induction in mice have been demonstrated when GluA1 phosphorylation through CaMKII and PKA molecules is inhibited through mutation (Lee et al., 2003). The mutant mice additionally showed significant spatial memory deficits (Lee et al., 2003). Furthermore, it has been shown that AMPA receptor trafficking

has a role in LTP and LTD. In the CA3-CA1 hippocampal synapse, overall movement of AMPA receptors to the postsynaptic membrane results in LTP while internalization of receptors contributes to LTD (Lee et al., 2004). Our data shows that baseline GluA1 subunit density is similar amongst male and female rats, unlike the baseline differences in GluN1. Previous studies have used antibody labeling to localize AMPA receptors in the CA3 of the male rat hippocampus, and found receptors prevalent in the somata and basal dendrites of the CA3 pyramidal cells (Vissavajjhala et al., 1996). Through post-embedding immunogold localization, the GluR2 subunit of AMPA was found to be colocalized with NMDA receptors in the CA1 dendrites and spines of male Sprague-Dawley rats (He et al., 1998). It has been previously shown that with estradiol stimulation, GluR2/3 subunit levels increase in female rat hypothalami compared to males, while GluA1 levels were the same between male and female rats (Diano et al., 1997; Rousseaux, 2008). While our study used rat hippocampi, this is further evidence that baseline GluA1 subunit densities may be the same between male and female rats. Furthermore, most previous studies of hippocampal AMPA distribution utilized only male rats (Takumi et al., 1999; Fux et al., 2003; Nyíri et al., 2003), and thus our study may be one of the only to offer a comparison of baseline GluA1 receptor subunit hippocampal density between males and females.

7.2. Effect of Oxy CPP on glutamate receptor subunit distributions

The current study shows that Oxy CPP altered the distribution of GluN1 receptor subunits within CA3 dendrites in females but had little effect on males (Fig. 15). With Oxy CPP, GluN1 near the plasma

Glutamate receptor	Region	Saline CPP		Oxy CPP		Saline CIS CPP		Oxy CIS CPP	
		female	male	female	male	female	male	female	male
GluN1s in CA3 pyramidal cell dendrites	On/μm	=				=			⬆
	Near/μm	=		⬇		=			⬆
	Cyto/μm²	>		⬇		>			⬆
	Total/μm²	>		⬇		>			⬆
GluN1 Spines	MF-CA3	=				=			
GluN1 Spines	CA3 SR	=				=			⬆
GluA1s in CA3 pyramidal cell dendrites	On/μm	=				=			
	Near/μm	=				=			
	Cyto/μm²	=				=			⬆
	Total/μm²	=				=			⬆
GluA1 Spines	MF-CA3	=				=			
GluA1 Spines	CA3 SR	=				<			

Fig. 15. Summary diagram: sex differences in glutamate receptor subunit distribution in the hippocampal CA3 region. At baseline, Sal-females compared to Sal-males had greater densities of cytoplasmic and total GluN1 in CA3 pyramidal cell dendrites. Similarly, CIS Sal-females compared to CIS Sal-males had greater densities of cytoplasmic and total GluN1 in CA3 pyramidal cell dendrites. In contrast, there were no baseline differences in GluA1 in Sal-females compared to Sal-males in CA3 pyramidal cell dendrites or spines. Moreover, CIS Sal-females compared to CIS Sal-males had no baseline differences in GluA1 in CA3 pyramidal cell dendrites. However, unlike GluN1, GluA1 was lower in spines in CIS Sal-females compared to CIS Sal-males. Following Oxy CPP, GluN1 decreased near the plasma membrane, in the cytoplasm and in total in CA3 pyramidal cell dendrites in females only. In contrast, CIS Oxy-males (which did not acquire CPP) had elevated GluN1 and GluA1 in several compartments in CA3 pyramidal cell dendrites. CIS Oxy-males also had elevated numbers of GluN1-labeled spines in SR.

membrane, in the cytoplasm, and in total decreased in dendrites of female rats. Interestingly, although the total number of GluN1 subunits was reduced, Oxy CPP decreased the density of GluN1 subunits to be essentially equivalent to the density of GluN1 evident in male rats. As discussed previously, female rats had higher baseline levels of GluN1, and thus we see that Oxy CPP resulted in an approximately equal density of GluN1 subunits between females and males. In contrast, there were no changes in the distribution of GluA1 in female or male rats following Oxy CPP, from similar baseline levels in both sexes.

Our previous studies have shown that Oxy CPP primes rats, particularly females, to have enhanced opioid learning and susceptibility to addictive learning behaviors (Ryan et al., 2018). Our other past work demonstrated that Oxy CPP leads to an increase in opioid, stress, and plasticity signaling molecules (such as ARC) in the hippocampus of female rats, contributing to LTP learning processes, synaptic plasticity, and memory (Randesi et al., 2019). While the current data shows a decrease in baseline GluN1 receptor subunit density in the CA3 hippocampus of female rats following Oxy CPP, this does not discount the previous evidence of Oxy CPP enhancing addictive learning behaviors in females, but may suggest a mechanism at play other than glutamatergic signaling in the CA3 pyramidal cell dendrites.

One mechanism that may explain these results is glutamatergic signaling in CA3 dendritic spines. While Oxy CPP did not significantly alter total levels of GluN1 amongst females and male dendrites, it did change the distribution of GluN1 in spinal compartments. Oxy-female rats compared to Sal-female rats have a greater proportion of GluN1 labeling in the cytoplasm of spines in both the SR and SLu. Interestingly, our previous study showed that Oxy CPP does not significantly alter delta opioid receptor (DOR) distribution in the CA3 hippocampal spines of male and female rats (Chalangal et al., 2021). This contrasts with our current study in which Oxy CPP causes redistribution of GluN1 and GluA1 in CA3 spines, which may be significant in regards to increasing excitability and synaptic neuroplasticity.

The redistribution of GluN1 subunits in dendritic spines supports processes promoting glutamatergic plasticity. NMDA subunits are known to be involved in the development of dendritic spines and maintenance of the cellular cytoskeleton (Akashi et al., 2009). The GluN1 and GluN2B subunits bind to an actin-binding protein, α-actinin, which functions to regulate the morphology of dendritic spines (Akashi et al., 2009). Subsequently, it has been shown that LTP is associated with an increase of actin filament in dendritic spines, and that the actin filament component is dependent on activation of the NMDA receptor (Fukazawa et al., 2003). Thus, we postulate that increases in GluN1 in SR dendritic spines seen in CIS Oxy-females may facilitate plasticity processes needed for the acquisition to opioid-associative learning behaviors.

7.3. Effect of CIS on glutamate receptor subunit distributions

Stress is known to disrupt vital hippocampal functions like learning and memory (Kim and Diamond, 2002; Lutz and Kieffer, 2013). In the present study, following CIS, GluN1 receptor subunits redistributed away from the plasma membrane into the cytoplasm of CA3 dendrites in female and male rats (Fig. 15). We also found that unstressed and stressed females have higher levels of GluN1 than US and CIS males, respectively. In SR and SLu spines, there is a decrease in GluN1 in females and males following CIS. In both sexes, the total number of GluN1 subunits increased in CA3 dendrites following CIS. Our data echoes the findings of others (Sun et al., 2020), who showed that the total protein and mRNA levels of GluN1, GluN2A, and GluN2B were significantly increased in the CA3 region of the hippocampus in male Sprague Dawley rats exposed to repeated restraint stress (RRS) when compared to control. Additionally, the same experiment showed that the dendritic spine density in the CA3 region significantly decreased and that LTP was attenuated in male rats exposed to RRS (Sun et al., 2020).

In regard to AMPA receptors, males had an increase in GluA1 on the

plasma membrane and in total with a slight decrease in dendritic cytoplasm in small CA3 dendrites whereas females had no changes in GluA1 levels in response to stress. This suggests that CIS caused increased trafficking of GluA1 receptor subunits to the surface of dendrites in male rats, but did not have the same impact in females. Taken together, our data suggests that CIS creates alternate trafficking patterns of glutamate receptor subunits in the male hippocampus. Previous literature has also indicated differences in NMDA and AMPA receptor activation following stress. One study using whole-cell patch-clamp technique on rat hippocampal CA3 synapses showed that stress resulted in an increase deactivation time-constant and amplitude of excitatory postsynaptic currents (EPSCs) mediated by NMDA receptors, but no effect on AMPA mediated EPSCs (Kole et al., 2002), mimicking the significant change our data shows in GluN1 receptor subunit density with less change in GluA1. It is well-known that stress alters the morphology of hippocampal dendrites and even inhibits neurogenesis in the brain, both of which affect synaptic plasticity and memory (Kim and Diamond, 2002). Chronic stress reconfigures the brain in a neuroprotective fashion; specifically, it causes dendritic retraction with a simultaneous loss of synapses in susceptible areas of the brain such as the hippocampus, medial prefrontal cortex, and medial amygdala, which in turn alters neuroendocrine and behavioral functions that are necessary for the organism to cope with the chronic stressor (McEwen and Akil, 2020). Other studies have shown that chronic stress impacts the CA1 hippocampus by reducing density of dendritic spines, causing atrophy of the region (Sandi and Pinelo-Nava, 2007) and reducing LTP (Bhagya et al., 2017). There are several molecular mediators that contribute to adaptive plasticity, including BDNF, FGF2, IGF-1 (McEwen and Akil, 2020). Our results thus add to the ongoing conversation about adaptive plasticity by supporting a mechanism in how stress impacts dendritic morphology and function through glutamate receptor subunit trafficking.

Previous studies have analyzed the effect of RRS on both NMDA receptor protein levels and glutamate levels. RRS results in an increase in NMDA receptor protein level in the male rat hippocampus (Sun et al., 2020). Using *in vivo* microdialysis, it has been previously demonstrated that ten days of RRS results in lower glutamate levels in the male rat hippocampus compared to unstressed controls (Macht et al., 2020). Even though prior studies have shown that RRS reduces glutamate levels in the male rat hippocampus, our study offers a different perspective by suggesting that the increase in GluN1 in all cellular compartments in male rats following CPP behaviors and CIS potentially increases the availability of receptors to bind glutamate, similar to Sun et al. (2020). Such a process may impact the lack of opioid receptor redistribution seen in our prior experiments in CIS males (Reich et al., 2019).

7.4. Effect of CIS plus Oxy on glutamate receptor subunit distributions

It is important to note that male rats subjected to CIS did not acquire Oxy CPP as evidenced in our prior experiment (Reich et al., 2019). In Oxy-males, CIS increased GluN1 density in all dendritic compartments and spines as well as GluA1 density in the cytoplasm and in total (Fig. 15). In CIS females, Oxy CPP increased the ratio of GluA1 on the plasma membrane of dendrites without altering GluN1 density. In female spines, although total levels remained the same, Oxy CPP redistributed GluN1 and GluA1 from the cytoplasm to near the plasma membrane, creating an increased pool of available glutamate receptors ready to be transported to the membrane. Overall, CIS and Oxy CPP had a greater impact on male rats with little effect on females.

Our previous study showed that CIS Oxy CPP redistributes opioid receptors (DORs) in the CA3 region of the hippocampus to enhance neuroplasticity and excitability (Chalangal et al., 2021). Whereas the current study showed no difference in GluN1 or GluA1 levels between CIS Sal-females and CIS Oxy-females, our past study showed CIS Oxy-females had higher levels of DOR densities in CA3 synapses than CIS Sal-females, which promote opioid-mediated LTP (Chalangal et al., 2021). This difference may suggest that CIS and Oxy CPP protect the

hippocampal opioid receptor system in females in a maladaptive way that primes reward-related learning processes while maintaining glutamate receptor levels to potentially avoid glutamate induced-excitation of dendrites. On the other hand, while male rats did not have changes in opioid receptors following CIS Oxy CPP (Chalangal et al., 2021), they had increased GluN1 and GluA1 receptor subunit density. This proposes an opposite alteration in opioid and glutamate receptors between male and female rats, suggesting that when Oxy CPP is acquired (as it is in females), hippocampal glutamate subunit receptor density is not impacted potentially to avoid glutamate-induced excitation in hippocampal cells.

7.5. Functional implications

The current study builds upon previous work that has established the sex-dependent differences in the hippocampal opioid system (Chalangal et al., 2021). We offer a depiction of baseline GluN1 and GluA1 receptor subunit densities in female and male rat CA3 hippocampi, as well as the effects of CIS and Oxy CPP on receptor subunit density and distribution in CA3 pyramidal cells and dendritic spines. Our study revealed that Oxy CPP alone decreases GluN1 density in CA3 pyramidal cell dendrites in females whereas CIS combined with behavior in males increases GluN1 and GluA1 density, creating an increased pool of glutamate receptors available for ligand binding. Along with our prior studies, these results suggest that glutamate receptor subunit trafficking in the hippocampus is sex-dependent, and although CIS and behavior may increase sensitivity to glutamate in males, females are not affected in the same way. Furthermore, this potential increase in glutamate sensitivity in CIS male rats may contribute to the lack of opioid receptor redistribution and may potentially be responsible for the diminished capacity to acquire Oxy CPP. Whereas our previous studies indicated that CIS and Oxy CPP redistributes opioid receptors in the female hippocampus to promote opioid-associative learning processes, we have demonstrated here that glutamate receptors densities do not change dramatically. Nonetheless, it is interesting to note the shift of GluN1 and GluA1 in female spines from the cytoplasm of the spine to the plasmalemma following CIS Oxy CPP. This may suggest that dendritic spines contribute to opioid-associative learning in females through glutamate receptor subunit trafficking.

One of the most serious public health crises in the United States, the opioid epidemic continues to worsen as opioid overdose death rates rise (Volkow and Blanco, 2021). Women are especially susceptible as it has been shown that females are more likely to misuse prescription opioids for pain management and anxiety than males (NIDA, 2021). Females additionally progress to drug dependence quicker, are less likely to seek treatment for addiction than men, and endure higher levels of craving and relapse during abstinence [reviewed in (Bobzean et al., 2014)]. The sex-dependent differences found in the current study may be relevant on the larger scale of sex-dependent differences in opioid addiction. For example, hormone levels and menstrual cycle phase have been suggested to be an important consideration in both forming and reducing cue induced craving in women (American Addiction Centers, 2020). It has been shown that in the follicular phase of the menstrual cycle, where estrogen levels are increasing, women have greater subjective responses to cocaine (Bobzean et al., 2014). Administration of progesterone decreases some positive subjective effects of cocaine (Bobzean et al., 2014). Thus, as hormone levels impact the hippocampal opioid system (Chalangal et al., 2021), glutamate receptor subunit densities may potentially play a role in these processes as well, an interesting area of future study.

Additionally, the interaction between opioid addiction and biological stress is a growing field of interest. Stress is an ongoing body process that helps organisms adapt to the environment to maintain homeostasis through various mediators, a term known as allostasis (McEwen and Akil, 2020). But if environmental stressors are chronic, it can be toxic to overall health as mediators become overly activated and/or

dysregulated (McEwen and Akil, 2020). The hippocampus is critically involved in neuroendocrine regulation of stress hormones and memory (Kim and Diamond, 2002). We are the first study to show that glutamate subunit receptor trafficking in the hippocampus is affected by chronic stress and Oxy CPP in a sex-dependent manner, and previous studies suggest that redistribution and over-activation of glutamate receptors results in retraction of dendrites (McEwen and Akil, 2020). This appropriate response to stress becomes maladaptive when the stressor is chronic (CIS in this study), as evidenced by female acquisition of Oxy CPP behaviors. Our study thus offers a potential molecular explanation for how chronic stress impacts the hippocampal neural network and subsequently drug-seeking behaviors differently between males and females.

The current study also adds to the growing body of literature studying the molecular mechanisms of stress and their impact in clinical diseases, especially psychiatric and neurologic disorders. Dysregulation and further maladaptation of normal stress mechanisms includes increased sensitivity to menacing stimuli coupled with a lack of response termination, leading to a discrepancy between internal homeostasis and the outside world (McEwen and Akil, 2020). This dichotomy is seen in mood shifts that characterize bipolar disorder or decreased overall mood of major depressive disorder (McEwen and Akil, 2020). Additionally, male rat models of Gulf War Illness, which includes confusion, irritability, somnolence, fatigue, and memory loss, suggest that stress in combination with an anti-nerve agent interact to cause such symptoms (Macht et al., 2020). Personal response to environmental stressors also has been shown to impact one's susceptibility to psychiatric disorders (Akil et al., 2018). Research has shown that toxic environmental stressors, such as poverty, affect development of pediatric brain structures and cause dysregulation in the physiological stress response (McEwen and McEwen, 2017). Without proper counterbalancing forces, such as nurturing relationships and social networks, the effects of toxic stress manifest in poor executive function as well as illnesses like asthma, diabetes, depression, and cardiovascular disease [as reviewed in (McEwen and McEwen, 2017)]. While MRI imaging has revealed that toxic stress results in decreased volume of the hippocampus, it has also been shown that positive activities, such as intense learning, cause an increase in gray matter volume of the hippocampus, important in mediating resilience to stress (Draganski et al., 2006; McEwen and Akil, 2020).

Despite the above mentioned impacts of chronic stress, females still possessed an ability to associate Oxy with cue learning behaviors. Males on the other hand, which had an increase in glutamate subunit receptor density in CA3 pyramidal neurons, have a lack of plasticity after CIS as evidenced by their inability to acquire Oxy CPP. This potentially indicates that males may have less of an ability to perform drug-cue associative learning after chronic stress. This adds to our previous studies that have shown the hippocampal mechanisms in place after chronic stress are different in promoting and disrupting drug associative learning between males and females (Chalangal et al., 2021). Taken together, the results of this study may offer molecular insight into why females experience dependence, cravings, and relapse differently than males (Bobzean et al., 2014).

In sum, stress and cue-related drug exposure differentially impact the hippocampal opioid system between females and males. Our study is the first to show the potential involvement of glutamate receptor subunit trafficking in CA3 pyramidal cells in these processes. Further research is necessary to elucidate the connection between the effects of stress on hippocampal opioid circuits and the impact on drug dependence risk.

Commemoration

Bruce McEwen and the discovery of estrogen receptor alpha in hippocampal dendritic spines (by Teresa Milner). It started with a question: "I don't understand why estrogen receptors can't be on membranes like other receptors?" Although I thought this was a naïve

question at the time, Bruce did not. In fact, he responded that this was a great question and that there was evidence estrogen receptor alpha (ERα) could be on membranes. He then went on to state that this question could probably be answered with immuno-electron microscopy and that he had a specific antibody to ERα he could give me to test the possibility. He also paired me with Steve Alves to collaborate on the project. A few months later, Steve and I approached Bruce with micrographs in hand, clearly showing the localization of ERα in hippocampal dendritic spines. Bruce nearly fell off his chair he was so excited! He then proceeded to enthusiastically plan the next steps. This experiment resulted in a collaboration of our two labs that spanned several decades. It was instrumental in changing the direction of both of our labs in studying the mechanisms of membrane steroid receptors in the hippocampus. Additionally, it resulted in numerous collaborative studies especially those aimed at understanding the role of sex and stress on the hippocampal opioid system. One of these studies is presented in this special issue. Bruce was my mentor, collaborator and friend who greatly impacted the way I approached science. In particular, Bruce's urging to see the "Big picture" of the data is something that I will carry with me always. Additionally, his vision of mentored group science will continue to inspire me.

Author contributions

T.A.M., M.J.K. and B.S.M. obtained funding for project; A.D., T.A.M., M.J.K. and B.S.M. designed research; A.D., M.J., K.F., Y.Z., and T.A.M. performed research; A.D., M.J., K.F. analyzed data; A.D., M.J., L.S. and T.A.M., wrote the paper.

Declaration of competing interest

The authors declare no competing financial interests.

Acknowledgements

References

Akashi, K., Kakizaki, T., Kamiya, H., Fukaya, M., Yamasaki, M., Abe, M., Natsume, R., Watanabe, M., Sakimura, K., 2009. NMDA receptor GluN2B (GluR epsilon 2/NR2B) subunit is crucial for channel function, postsynaptic macromolecular organization, and actin cytoskeleton at hippocampal CA3 synapses. J. Neurosci. 29, 10869–10882.

Akil, H., Gordon, J., Hen, R., Javitch, J., Mayberg, H., McEwen, B., Meaney, M.J., Nestler, E.J., 2018. Treatment resistant depression: a multi-scale, systems biology approach. Neurosci. Biobehav. Rev. 84, 272–288.

American Addiction Centers, 2020. How Hormones Affect Addiction. American Addiction Centers.

Ashirova, E., Contoreggi, N.H., Johnson, M.A., Al-Khayat, F.J., Calcano, G.A., Rubin, B. R., O'Cinneide, E.M., Zhang, Y., Zhou, Y., Gregoire, L., McEwen, B.S., Kreek, M.J., Milner, T.A., 2021. Oxycodone injections not paired with conditioned place preference have little effect on the hippocampal opioid system in female and male rats. Synapse 75, e22182.

Barkóczi, B., Juhász, G., Averkin, R.G., Vörös, I., Vertes, P., Penke, B., Szegedi, V., 2012. GluA1 phosphorylation alters evoked firing pattern in vivo. Neural Plast 2012 286215.

Bear, M.F., Malenka, R.C., 1994. Synaptic plasticity: LTP and LTD. Curr. Opin. Neurobiol. 4, 389–399.

Becker, J.B., Chartoff, E., 2019. Sex differences in neural mechanisms mediating reward and addiction. Neuropsychopharmacology 44, 166–183.

Becker, J.B., McClellan, M.L., Reed, B.G., 2017. Sex differences, gender and addiction. J. Neurosci. Res. 95, 136–147.

Beckerman, M.A., Glass, M.J., 2011. Ultrastructural relationship between the AMPA-GluR2 receptor subunit and the mu-opioid receptor in the mouse central nucleus of the amygdala. Exp. Neurol. 227, 149–158.

Beckerman, M.A., Glass, M.J., 2012. The NMDA-NR1 receptor subunit and the mu-opioid receptor are expressed in somatodendritic compartments of central nucleus of the amygdala neurons projecting to the bed nucleus of the stria terminalis. Exp. Neurol. 234, 112–126.

Bellamy, J.R., Rubin, B.R., Zverovich, A., Zhou, Y., Contoreggi, N.H., Gray, J.D., McEwen, B.S., Kreek, M.J., Milner, T.A., 2019. Sex and chronic stress differentially alter phosphorylated mu and delta opioid receptor levels in the rat hippocampus following oxycodone conditioned place preference. Neurosci. Lett. 713, 134514.

Bhagya, V.R., Srikumar, B.N., Veena, J., Shankaranarayana Rao, B.S., 2017. Short-term exposure to enriched environment rescues chronic stress-induced impaired hippocampal synaptic plasticity, anxiety, and memory deficits. J. Neurosci. Res. 95, 1602–1610.

Billa, S.K., Liu, J., Bjorklund, N.L., Sinha, N., Fu, Y., Shinnick-Gallagher, P., Morón, J.A., 2010. Increased insertion of glutamate receptor 2-lacking alpha-amino-3-hydroxy-5-methyl-4-isoxazole propionic acid (AMPA) receptors at hippocampal synapses upon repeated morphine administration. Mol. Pharmacol. 77, 874–883.

Bliss, T.V., Collingridge, G.L., 1993. A synaptic model of memory: long-term potentiation in the hippocampus. Nature 361, 31–39.

Bobzean, S.A., DeNobrega, A.K., Perrotti, L.I., 2014. Sex differences in the neurobiology of drug addiction. Exp. Neurol. 259, 64–74.

Boudin, H., Pelaprat, D., Rostene, W., Pickel, V.M., Beaudet, A., 1998. Correlative ultrastructural distribution of neurotensin receptor proteins and binding sites in the rat substantia nigra. J. Neurosci. : Off. J.Soc. Neurosci. 18, 8473–8484.

Brose, N., Huntley, G.W., Stern-Bach, Y., Sharma, G., Morrison, J.H., Heinemann, S.F., 1994. Differential assembly of coexpressed glutamate receptor subunits in neurons of rat cerebral cortex. J. Biol. Chem. 269, 16780–16784.

Celio, M.R., 1990. Calbindin D-28k and parvalbumin in the rat nervous system. Neuroscience 35, 375–475.

Celio, M.R., Baier, W., Scharer, L., de Viragh, P.A., Gerday, C., 1988. Monoclonal antibodies directed against the calcium binding protein parvalbumin. Cell Calcium 9, 81–86.

Chalangal, J., Mazid, S., Windisch, K., Milner, T.A., 2021. Sex differences in the rodent hippocampal opioid system following stress and oxycodone associated learning processes. Pharmacol., Biochem. Behav. 212, 173294.

Collins, D., Reed, B., Zhang, Y., Kreek, M.J., 2016. Sex differences in responsiveness to the prescription opioid oxycodone in mice. Pharmacol., Biochem. Behav. 148, 99–105.

Daniel, J.M., Dohanich, G.P., 2001. Acetylcholine mediates the estrogen-induced increase in NMDA receptor binding in CA1 of the hippocampus and the associated improvement in working memory. J. Neurosci. 21, 6949–6956.

Deutsch-Feldman, M., Picetti, R., Seip-Cammack, K., Zhou, Y., Kreek, M.J., 2015. Effects of handling and vehicle injections on adrenocorticotropic and corticosterone concentrations in Sprague-Dawley compared with Lewis rats. J. Am. Assoc. Lab. Anim. Sci : JAALAS 54, 35–39.

Diano, S., Naftolin, F., Horvath, T.L., 1997. Gonadal steroids target AMPA glutamate receptor-containing neurons in the rat hypothalamus, septum and amygdala: a morphological and biochemical study. Endocrinology 138, 778–789.

Draganski, B., Gaser, C., Kempermann, G., Kuhn, H.G., Winkler, J., Büchel, C., May, A., 2006. Temporal and spatial dynamics of brain structure changes during extensive learning. J. Neurosci. 26, 6314–6317.

Drake, C.T., Chavkin, C., Milner, T.A., 2007. Opioid systems in the dentate gyrus. Prog. Brain Res. 163, 245–263.

Fernandez-Monreal, M., Brown, T.C., Royo, M., Esteban, J.A., 2012. The balance between receptor recycling and trafficking toward lysosomes determines synaptic strength during long-term depression. J. Neurosci. 32, 13200–13205.

Frey, M.C., Sprengel, R., Nevian, T., 2009. Activity pattern-dependent long-term potentiation in neocortex and hippocampus of GluA1 (GluR-A) subunit-deficient mice. J. Neurosci. 29, 5587–5596.

Fukazawa, Y., Saitoh, Y., Ozawa, F., Ohta, Y., Mizuno, K., Inokuchi, K., 2003. Hippocampal LTP is accompanied by enhanced F-actin content within the dendritic spine that is essential for late LTP maintenance in vivo. Neuron 38, 447–460.

Fux, C.M., Krug, M., Dityatev, A., Schuster, T., Schachner, M., 2003. NCAM180 and glutamate receptor subtypes in potentiated spine synapses: an immunogold electron microscopic study. Mol. Cell. Neurosci. 24, 939–950.

Glass, M.J., Kruzich, P.J., Kreek, M.J., Pickel, V.M., 2004. Decreased plasma membrane targeting of NMDA-NR1 receptor subunit in dendrites of medial nucleus tractus solitarius neurons in rats self-administering morphine. Synapse 53, 191–201.

Glass, M.J., Kruzich, P.J., Colago, E.E., Kreek, M.J., Pickel, V.M., 2005. Increased AMPA GluR1 receptor subunit labeling on the plasma membrane of dendrites in the basolateral amygdala of rats self-administering morphine. Synapse 58, 1–12.

Glass, M.J., Hegarty, D.M., Oselkin, M., Quimson, L., South, S.M., Xu, Q., Pickel, V.M., Inturrisi, C.E., 2008. Conditional deletion of the NMDA-NR1 receptor subunit gene in the central nucleus of the amygdala inhibits naloxone-induced conditioned place aversion in morphine-dependent mice. Exp. Neurol. 213, 57–70.

Gould, E., Woolley, C.S., Frankfurt, M., McEwen, B.S., 1990. Gonadal steroids regulate dendritic spine density in hippocampal pyramidal cells in adulthood. J. Neurosci. 10, 1286–1291.

Haberstock-Debic, H., Wein, M., Barrot, M., Colago, E.E., Rahman, Z., Neve, R.L., Pickel, V.M., Nestler, E.J., von Zastrow, M., Svingos, A.L., 2003. Morphine acutely regulates opioid receptor trafficking selectively in dendrites of nucleus accumbens neurons. J. Neurosci. : Off. J.Soc. Neurosci. 23, 4324–4332.

Hardingham, G.E., Bading, H., 2010. Synaptic versus extrasynaptic NMDA receptor signalling: implications for neurodegenerative disorders. Nat. Rev. Neurosci. 11, 682–696.

Harte-Hargrove, L.C., Maclusky, N.J., Scharfman, H.E., 2013. Brain-derived neurotrophic factor-estrogen interactions in the hippocampal mossy fiber pathway: implications for normal brain function and disease. Neuroscience 239, 46–66.

Harte-Hargrove, L.C., Varga-Wesson, A., Duffy, A.M., Milner, T.A., Scharfman, H.E., 2015. Opioid receptor-dependent sex differences in synaptic plasticity in the hippocampal mossy fiber pathway of the adult rat. J. Neurosci.: Off. J. Soc.Neurosci. 35, 1723–1738.

Hayashi, Y., Shi, S.H., Esteban, J.A., Piccini, A., Poncer, J.C., Malinow, R., 2000. Driving AMPA receptors into synapses by LTP and CaMKII: requirement for GluR1 and PDZ domain interaction. Science 287, 2262–2267.

He, Y., Janssen, W.G., Morrison, J.H., 1998. Synaptic coexistence of AMPA and NMDA receptors in the rat hippocampus: a postembedding immunogold study. J. Neurosci. Res. 54, 444–449.

Heinsbroek, J.A., De Vries, T.J., Peters, J., 2020. Corrigendum: glutamatergic systems and memory mechanisms underlying opioid addiction. Cold Spring Harb Perspect Med 10.

Hou, Y.Y., Liu, Y., Kang, S., Yu, C., Chi, Z.Q., Liu, J.G., 2009. Glutamate receptors in the dorsal hippocampus mediate the acquisition, but not the expression, of conditioned place aversion induced by acute morphine withdrawal in rats. Acta Pharmacol. Sin. 30, 1385–1391.

Hussain, N.K., Thomas, G.M., Luo, J., Huganir, R.L., 2015. Regulation of AMPA receptor subunit GluA1 surface expression by PAK3 phosphorylation. Proc. Natl. Acad. Sci. U. S. A. 112, E5883–E5890.

Johnson, M.A., Contoreggi, N.H., Kogan, J.F., Bryson, M., Rubin, B.R., Gray, J.D., Kreek, M.J., McEwen, B.S., Milner, T.A., 2020. Chronic stress differentially alters mRNA expression of opioid peptides and receptors in the dorsal hippocampus of female and male rats. J. Comp. Neurol.

Kesner, R.P., Warthen, D.K., 2010. Implications of CA3 NMDA and opiate receptors for spatial pattern completion in rats. Hippocampus 20, 550–557.

Kim, J.J., Diamond, D.M., 2002. The stressed hippocampus, synaptic plasticity and lost memories. Nat. Rev. Neurosci. 3, 453–462.

Kole, M.H., Swan, L., Fuchs, E., 2002. The antidepressant tianeptine persistently modulates glutamate receptor currents of the hippocampal CA3 commissural associational synapse in chronically stressed rats. Eur. J. Neurosci. 16, 807–816.

Koob, G.F., Volkow, N.D., 2010. Neurocircuitry of addiction. Neuropsychopharmacology : Off. Publ. Am. Coll. Neuropsychopharmacol. vol. 35, 217–238.

Lacy, R.T., Strickland, J.C., Feinstein, M.A., Robinson, A.M., Smith, M.A., 2016. The effects of sex, estrous cycle, and social contact on cocaine and heroin self-administration in rats. Psychopharmacology 233, 3201–3210.

Ladépêche, L., Dupuis, J.P., Groc, L., 2014. Surface trafficking of NMDA receptors: gathering from a partner to another. Semin. Cell Dev. Biol. 27, 3–13.

Lee, H.K., Takamiya, K., Han, J.S., Man, H., Kim, C.H., Rumbaugh, G., Yu, S., Ding, L., He, C., Petralia, R.S., Wenthold, R.J., Gallagher, M., Huganir, R.L., 2003. Phosphorylation of the AMPA receptor GluR1 subunit is required for synaptic plasticity and retention of spatial memory. Cell 112, 631–643.

Lee, S.H., Simonetta, A., Sheng, M., 2004. Subunit rules governing the sorting of internalized AMPA receptors in hippocampal neurons. Neuron 43, 221–236.

Lutz, P.E., Kieffer, B.L., 2013. Opioid receptors: distinct roles in mood disorders. Trends Neurosci. 36, 195–206.

Macht, V.A., Woodruff, J.L., Burzynski, H.E., Grillo, C.A., Reagan, L.P., Fadel, J.R., 2020. Interactions between pyridostigmine bromide and stress on glutamatergic neurochemistry: insights from a rat model of Gulf War Illness. Neurobiol Stress 12, 100210.

Mazid, S., Hall, B.S., Odell, S.C., Stafford, K., Dyer, A.D., Van Kempen, T.A., Selegean, J., McEwen, B.S., Waters, E.M., Milner, T.A., 2016. Sex differences in subcellular distribution of delta opioid receptors in the rat hippocampus in response to acute and chronic stress. Neurobiology of Stress 5, 37–53.

McEwen, B.S., Milner, T.A., 2017. Understanding the broad influence of sex hormones and sex differences in the brain. J. Neurosci. Res. 95, 24–39.

McEwen, B.S., Akil, H., 2020. Revisiting the stress concept: implications for affective disorders. J. Neurosci. 40, 12–21.

McEwen, C.A., McEwen, B.S., 2017. Social structure, adversity, toxic stress, and intergenerational poverty: an early childhood model. Annu. Rev. Sociol. 43, 445–472.

Meilandt, W.J., Barea-Rodriguez, E., Harvey, S.A., Martinez Jr., J.L., 2004. Role of hippocampal CA3 mu-opioid receptors in spatial learning and memory. J. Neurosci.: Off. J. Soc.Neurosci. 24, 2953–2962.

Milner, T.A., Drake, C.T., 2001. Ultrastructural evidence for presynaptic mu opioid receptor modulation of synaptic plasticity in NMDA-receptor-containing dendrites in the dentate gyrus. Brain Res. Bull. 54, 131–140.

Milner, T.A., Waters, E.M., Robinson, D.C., Pierce, J.P., 2011. Degenerating processes identified by electron microscopic immunocytochemical methods. In: Manfredi, G., Kawamata, H. (Eds.), Neurodegeneration, Methods and Protocols. Springer, New York, pp. 23–59.

Mithani, S., Atmadja, S., Baimbridge, K.G., Fibiger, H.C., 1987. Neuroleptic-induced oral dyskinesias: effects of progabide and lack of correlation with regional changes in glutamic acid decarboxylase and choline acetyltransferase activities. Psychopharmacology (Berl) 93, 94–100.

NIDA, 2021. Sex and Gender Differences in Substance Use. https://www.drugabuse.gov/publications/research-reports/.

Nyíri, G., Stephenson, F.A., Freund, T.F., Somogyi, P., 2003. Large variability in synaptic N-methyl-D-aspartate receptor density on interneurons and a comparison with pyramidal-cell spines in the rat hippocampus. Neuroscience 119, 347–363.

Ordonez Gallego, A., Gonzalez Baron, M., Espinosa Arranz, E., 2007. Oxycodone: a pharmacological and clinical review. Clinical & Translational Oncology vol. 9,

298–307 official publication of the Federation of Spanish Oncology Societies and of the National Cancer Institute of Mexico.

Peters, A., Palay, S.L., Webster, H.d., 1991. The Fine Structure of the Nervous System: Neurons and Their Supporting Cells, 3 Edition. Oxford University Press, New York.

Pierce, J.P., Kelter, D.T., McEwen, B.S., Waters, E.M., Milner, T.A., 2014. Hippocampal mossy fiber leu-enkephalin immunoreactivity in female rats is significantly altered following both acute and chronic stress. J. Chem. Neuroanat. 55, 9–17.

Pierce, J.P., Kievits, J., Graustein, B., Speth, R.C., Iadecola, C., Milner, T.A., 2009. Sex differences in the subcellular distribution of AT(1) receptors and nadph oxidase subunits in the dendrites of C1 neurons in the rat rostral ventrolateral medulla. Neuroscience 163, 329–338.

Portugal, G.S., Al-Hasani, R., Fakira, A.K., Gonzalez-Romero, J.L., Melyan, Z., McCall, J.G., Bruchas, M.R., Morón, J.A., 2014. Hippocampal long-term potentiation is disrupted during expression and extinction but is restored after reinstatement of morphine place preference. J. Neurosci. 34, 527–538.

Pál, B., 2018. Involvement of extrasynaptic glutamate in physiological and pathophysiological changes of neuronal excitability. Cell. Mol. Life Sci. 75, 2917–2949.

Randesi, M., Zhou, Y., Mazid, S., Odell, S.C., Gray, J.D., Correa da Rosa, J., McEwen, B.S., Milner, T.A., Kreek, M.J., 2018. Sex differences after chronic stress in the expression of opioid- and neuroplasticity-related genes in the rat hippocampus. Neurobiology of Stress 8, 33–41.

Randesi, M., Contoreggi, N.H., Zhou, Y., Reich, B., Bellamy, J.R., Yu, F., Gray, J.D., McEwen, B.S., Milner, T.A., Kreek, M.J., 2019. Sex differences in neuroplasticity- and stress-related gene expression and protein levels in the rat Hippocampus following oxycodone conditioned place preference. Neuroscience.

Rebola, N., Srikumar, B.N., Mulle, C., 2010. Activity-dependent synaptic plasticity of NMDA receptors. J. Physiol. 588, 93–99.

Reich, B., Zhou, Y., Goldstein, E., Srivats, S.S., Contoreggi, N.H., Kogan, J.F., McEwen, B.S., Kreek, M.J., Milner, T.A., Gray, J.D., 2019. Chronic Immobilization Stress Primes the Hippocampal Opioid System for Oxycodone-Associated Learning in Female but Not Male rats. Synapse (New York, NY), e22088.

Ribeiro-Dasilva, M.C., Shinal, R.M., Glover, T., Williams, R.S., Staud, R., Riley 3rd, J.L., Fillingim, R.B., 2011. Evaluation of menstrual cycle effects on morphine and pentazocine analgesia. Pain 152, 614–622.

Rousseaux, C.G., 2008. A review of glutamate receptors II: pathophysiology and pathology. J. Toxicol. Pathol. 21, 133–173.

Rubin, B.R., Johnson, M.A., Berman, J.M., Goldstein, E., Pertsovskaya, V., Zhou, Y., Contoreggi, N.H., Dyer, A.G., Gray, J.D., Waters, E.M., McEwen, B.S., Kreek, M.J., Milner, T.A., 2020. Sex and chronic stress alter delta opioid receptor distribution within rat hippocampal CA1 pyramidal cells following behavioral challenges. Neurobiology of Stress.

Ryan, J.D., Zhou, Y., Contoreggi, N.H., Bshesh, F.K., Gray, J.D., Kogan, J.F., Ben, K.T., McEwen, B.S., Jeanne Kreek, M., Milner, T.A., 2018. Sex differences in the rat hippocampal opioid system after oxycodone conditioned place preference. Neuroscience 393, 236–257.

Saal, D., Dong, Y., Bonci, A., Malenka, R.C., 2003. Drugs of abuse and stress trigger a common synaptic adaptation in dopamine neurons. Neuron 37, 577–582.

Sandi, C., Pinelo-Nava, M.T., 2007. Stress and memory: behavioral effects and neurobiological mechanisms. Neural Plast 2007 78970.

Scavone, J.L., Asan, E., Van Bockstaele, E.J., 2011. Unraveling glutamate-opioid receptor interactions using high-resolution electron microscopy: implications for addiction-related processes. Exp. Neurol. 229, 207–213.

Scholl, L., Seth, P., Kariisa, M., Wilson, N., Baldwin, G., 2018. Drug and opioid-involved overdose deaths - United States, 2013-2017. MMWR Morb. Mortal. Wkly. Rep. 67, 1419–1427.

Shen, H.W., Scofield, M.D., Boger, H., Hensley, M., Kalivas, P.W., 2014. Synaptic glutamate spillover due to impaired glutamate uptake mediates heroin relapse. J. Neurosci. 34, 5649–5657.

Sheng, M., Kim, M.J., 2002. Postsynaptic signaling and plasticity mechanisms. Science 298, 776–780.

Siegel, S.J., Brose, N., Janssen, W.G., Gasic, G.P., Jahn, R., Heinemann, S.F., Morrison, J.H., 1994. Regional, cellular, and ultrastructural distribution of N-methyl-D-aspartate receptor subunit 1 in monkey hippocampus. Proc. Natl. Acad. Sci. U. S. A. 91, 564–568.

Siegel, S.J., Janssen, W.G., Tullai, J.W., Rogers, S.W., Moran, T., Heinemann, S.F., Morrison, J.H., 1995. Distribution of the excitatory amino acid receptor subunits GluR2(4) in monkey hippocampus and colocalization with subunits GluR5-7 and NMDAR1. J. Neurosci. 15, 2707–2719.

Sinha, R., 2007. The role of stress in addiction relapse. Curr. Psychiatr. Rep. 9, 388–395.

Sloviter, R.S., 1989. Calcium-binding protein (calbindin-D28k) and parvalbumin immunocytochemistry: localization in the rat hippocampus with specific reference to the selective vulnerability of hippocampal neurons to seizure activity. J. Comp. Neurol. 280, 183–196.

Sperk, G., Hamilton, T., Colmers, W.F., 2007. Neuropeptide Y in the dentate gyrus. Prog. Brain Res. 163, 285–297.

Strang, J., Volkow, N.D., Degenhardt, L., Hickman, M., Johnson, K., Koob, G.F., Marshall, B.D.L., Tyndall, M., Walsh, S.L., 2020. Opioid use disorder. Nat. Rev. Dis. Prim. 6, 3.

Sun, D.S., Zhong, G., Cao, H.X., Hu, Y., Hong, X.Y., Li, T., Li, X., Liu, Q., Wang, Q., Ke, D., Liu, G.P., Ma, R.H., Luo, D.J., 2020. Repeated restraint stress led to cognitive dysfunction by NMDA receptor-mediated hippocampal CA3 dendritic spine impairments in juvenile sprague-dawley rats. Front. Mol. Neurosci. 13, 552787.

Swanson, L.W., 1992. Brain Maps: Structure of the Rat Brain, 1 Edition. Elsevier, Amsterdam.

Takumi, Y., Ramírez-León, V., Laake, P., Rinvik, E., Ottersen, O.P., 1999. Different modes of expression of AMPA and NMDA receptors in hippocampal synapses. Nat. Neurosci. 2, 618–624.

Turner, C.D., Bagnara, J.T., 1971. General Endocrinology. W.B. Saunders, Philadelphia.

Tzschentke, T.M., Schmidt, W.J., 2003. Glutamatergic mechanisms in addiction. Mol. Psychiatr. 8, 373–382.

Van Kempen, T.A., Gorecka, J., Gonzalez, A.D., Soeda, F., Milner, T.A., Waters, E.M., 2014. Characterization of neural estrogen signaling and neurotrophic changes in the accelerated ovarian failure mouse model of menopause. Endocrinology 155, 3610–3623.

VanHouten, J.P., Rudd, R.A., Ballesteros, M.F., Mack, K.A., 2019. Drug overdose deaths among women aged 30-64 Years - United States, 1999-2017. MMWR Morbidity and mortality weekly report 68, 1–5.

Vissavajjhala, P., Janssen, W.G., Hu, Y., Gazzaley, A.H., Moran, T., Hof, P.R., Morrison, J. H., 1996. Synaptic distribution of the AMPA-GluR2 subunit and its colocalization with calcium-binding proteins in rat cerebral cortex: an immunohistochemical study using a GluR2-specific monoclonal antibody. Exp. Neurol. 142, 296–312.

Volkow, N.D., Blanco, C., 2021. The changing opioid crisis: development, challenges and opportunities. Mol. Psychiatr. 26, 218–233.

Walker, Q.D., Nelson, C.J., Smith, D., Kuhn, C.M., 2002. Vaginal lavage attenuates cocaine-stimulated activity and establishes place preference in rats. Pharmacol., Biochem. Behav. 73, 743–752.

Walker, Q.D., Cabassa, J., Kaplan, K.A., Li, S.T., Haroon, J., Spohr, H.A., Kuhn, C.M., 2001. Sex differences in cocaine-stimulated motor behavior: disparate effects of

gonadectomy. Neuropsychopharmacology : Off. Publ. Am. Coll. Neuropsychopharmacol. 25, 118–130.

Wang, H., Gracy, K.N., Pickel, V.M., 1999. Mu-opioid and NMDA-type glutamate receptors are often colocalized in spiny neurons within patches of the caudate-putamen nucleus. J. Comp. Neurol. 412, 132–146.

Woolley, C.S., Weiland, N.G., McEwen, B.S., Schwartzkroin, P.A., 1997. Estradiol increases the sensitivity of hippocampal CA1 pyramidal cells to NMDA receptor-mediated synaptic input: correlation with dendritic spine density. J. Neurosci. 17, 1848–1859.

Yokoi, N., Fukata, Y., Sekiya, A., Murakami, T., Kobayashi, K., Fukata, M., 2016. Identification of PSD-95 depalmitoylating enzymes. J. Neurosci.: Off. J. Soc. Neurosci. 36, 6431–6444.

Zamanillo, D., Sprengel, R., Hvalby, O., Jensen, V., Burnashev, N., Rozov, A., Kaiser, K. M., Köster, H.J., Borchardt, T., Worley, P., Lübke, J., Frotscher, M., Kelly, P.H., Sommer, B., Andersen, P., Seeburg, P.H., Sakmann, B., 1999. Importance of AMPA receptors for hippocampal synaptic plasticity but not for spatial learning. Science 284, 1805–1811.

Zhang, C., Li, S.S., Zhao, N., Yu, C., 2015. Phosphorylation of the GluN1 subunit in dorsal horn neurons by remifentanil: a mechanism for opioid-induced hyperalgesia. Genet. Mol. Res. 14, 1846–1854.

Zhang, J., Abdullah, J.M., 2013. The role of GluA1 in central nervous system disorders. Rev. Neurosci. 24, 499–505.